

1      **Large-scale optimal integration of wind and solar photovoltaic**  
2      **power in water-energy systems on islands**

3      Pedro Cabrera <sup>a,1</sup>, José Antonio Carta <sup>a</sup>, Henrik Lund <sup>b</sup>, Jakob Zinck Thellufsen <sup>b</sup>

4      <sup>a</sup> Department of Mechanical Engineering, University of Las Palmas de Gran Canaria, Campus  
5      de Tafira s/n, 35017 Las Palmas de Gran Canaria, Canary Islands, Spain.

6      <sup>b</sup> Department of Planning, Rendsburggade 14, Aalborg University, Denmark.

© 2021. This manuscript version is made available under the CC-BY-NC-ND 4.0  
license <http://creativecommons.org/licenses/by-nc-nd/4.0/>

*This document is the Accepted Manuscript version of a Published Work that  
appeared in final form in Energy Conversion and Management. To access the  
final edited and published work see <https://doi.org/10.1016/j.enconman.2021.113982>*

7

8      **Abstract**

9      This paper presents a new method based on the Smart Energy System concept to link the water  
10     infrastructure and the energy system of an island. The principal aim of this study is to determine  
11     whether this new method can increase the contribution of renewables (wind power and  
12     photovoltaic) to the primary energy supply of the island. The method considers water  
13     production and treatment systems as flexible loads and explores a wide range of possible water  
14     supply infrastructures and PV/wind power combinations in the search for an optimal energy-  
15     water configuration. The final optimal solution is based on a balance between energy fuel needs  
16     and energy excesses, CO<sub>2</sub> emissions, oil consumption, minimization of total annual costs and  
17     maximization of the renewable contribution. The proposed method increased the contribution  
18     of renewables from 5.14% to 24.6%. This corresponds to, on average, over 35% of the hourly  
19     electricity demand throughout 2018 being covered by renewables, against the current 6.6%.

---

<sup>1</sup> Corresponding author. tel.: +34 928 45 98 87; fax: +34 928 45 14 84

*E-mail address:* [pedro.cabrerasantana@ulpgc.es](mailto:pedro.cabrerasantana@ulpgc.es) (Pedro Cabrera)

20 The study reveals that wind technology integration is of fundamental importance for renewable  
21 exploitation in insular water-energy systems, with wind energy contributing more than 70% of  
22 the renewable participation in this case study.

23 **Keywords:** Renewable energy integration on islands; Energy-water planning; Pareto multi-objective  
24 optimization; Energy-water synergies; smart energy-water system approach.

## Nomenclature

EEP	Excess electricity production
ERDF	European Regional Development Fund
HRES	Hybrid renewable energy sources
ISTAC	Spanish initials: Canary Islands Institute of Statistics
$ip(i,j,k,m)$	Vector to save intersection points (Fig. 4).
MAE	Mean absolute error
MAPE	Mean absolute percentage error
O&M	Operation and Maintenance
PES	Primary energy supply
PHS	Pumped-hydroelectric storage
PV	Solar photovoltaic
$R^2$	R-Squared measure of agreement
REE	Spanish initials of the TSO in Spain: Red Eléctrica de España, S.A.U.
RES	Renewable energy sources
RO	Reverse osmosis
SCs	Synchronous compensators
SSE	Sum of squared errors

SSR	Sum of squared regression
SST	Sum of squared total
TSO	Transmission system operator
$x_1$	Water storage capacity. Decision variable (Fig. 4).
$x_2$	Water production capacity. Decision variable (Fig. 4).
$x_3$	Wind power installed in the system (in % to cover the total electricity demand with wind power). Decision variable (Fig. 4).
$x_4$	PV power installed in the system (in % to cover the total electricity demand with PV power). Decision variable (Fig. 4).
$x_{11}$	Current water storage capacity installed in the reference validated scenario. Lower constraint of $x_1$ (Fig. 4)
$x_{12}$	Current water production capacity installed in the reference validated scenario. Lower constraint of $x_2$ (Fig. 4)
$x_{13}$	Current wind power installed in the reference validated scenario (in % to cover the total electricity demand with wind power). Lower constraint of $x_3$ (Fig. 4)
$x_{14}$	Current PV power installed in the reference validated scenario (in % to cover the total electricity demand with PV power). Lower constraint of $x_4$ (Fig. 4)
$x_{11}$	Maximum feasible water storage capacity. Upper constraint of $x_1$ (Fig. 4)
$x_{12}$	Current water production capacity installed in the reference validated scenario. Upper constraint of $x_2$ (Fig. 4)
$x_{13}$	Current wind power installed in the reference validated scenario (in % to cover the total electricity demand with wind power). Upper constraint of $x_3$ (Fig. 4)
$x_{14}$	Current PV power installed in the reference validated scenario (in % to cover the total electricity demand with PV power). Upper constraint of $x_4$ (Fig. 4)

26 **1 Introduction**

27 Most islands around the world do not have enough natural water resources to cover all their  
28 hydric needs [1]. Consequently, they have to desalinate seawater to satisfy the fresh water  
29 demand [1–3]. Since desalination is an intensive electricity consumer [2], a water scarcity  
30 problem in islands is also an energy problem. The electricity demand to power water supply  
31 systems supported by desalination represents on average around 10% of the total electricity  
32 demand [3,4] in the respective energy systems. For this reason, the development of strategies  
33 to promote desalination powered by renewable energy sources (RES) is considered a question  
34 of growing importance for innumerable islands around the world, especially those without  
35 hydric resources [5]. Several authors have published studies which have addressed this question  
36 from different point of views, but generally linking the electricity and desalination sectors [3].  
37 Some of these studies have been carried out for relatively small islands. A very interesting and  
38 representative example of such studies is the one developed by Segurado et al. in the island of  
39 S. Vicente, in Cabo Verde [6]. In their study, these authors first analyse the relevant state-of-  
40 the-art and then propose two alternative scenarios to deal with the problem of excess wind  
41 energy production. The first scenario is based on sending the excess wind power directly to the  
42 desalination units. The second uses both desalination units and a pumped hydro storage (PHS)  
43 system to store this wind power excess. However, not all islands have a suitable topography for  
44 the installation of a PHS system. When no such possibility exists, another strategy needs to be  
45 considered aimed at directly linking renewable energy power plants and desalination units. In  
46 this respect, a lot of work has been conducted on modelling the combination of hybrid  
47 renewable energy sources (HRESs) and desalination plants. The models aim to optimally size  
48 the systems considering the energy demand rate and meteorological conditions [7]. Charcosset  
49 [8] reviewed a wide variety of RES-powered desalination systems which had been developed.  
50 Ma and Lu [9] carried out a specific review focused on the wind-desalination interrelation. They

51 concluded that wind power and reverse osmosis (RO) desalination technology was one of the  
52 most promising combinations in this field. This is at least partly because RO presents the lowest  
53 energy consumption in the desalination industry [4,6,10]. An additional reason is that RO  
54 facilities are usually located in coastal areas where the wind resource is frequently high. The  
55 Canary Islands (Spain) have lengthy and extensive experience in this field [11]. The reputation  
56 of these islands at European level in matters related to saline water desalination technologies  
57 and the management of scarce water resources is well known [12]. The number of desalination  
58 plants installed in the Canary Islands per head of population is high [11,12].

59 Through the use of Machine Learning tools, the latest advances in the desalination industry are  
60 facilitating the variable operation of desalination plants [10,13–15], converting them into  
61 potential flexible energy consumers. This raises new research questions about the linking of  
62 desalination and energy systems [16]. Additionally, the use of these techniques in the prediction  
63 of power generation in a wind farm is obtaining interesting results [17,18]. In this new scenario,  
64 a desalination plant could be designed to cover water needs whilst at the same time having  
65 specific energy goals in mind. Moreover, the flexibility of emerging technologies such as  
66 Artificial Intelligence should enable new and feasible energy-water nexus planning strategies.  
67 These approaches could be based on oversizing the desalination capacity of a region to integrate  
68 more renewables and increase the efficiency of the overall energy system. This is the initial  
69 hypothesis of this paper. More specifically, the objective of this research is to develop a new  
70 method for the optimal design of water-energy infrastructures which are able to cover energy  
71 and water demands and increase the contribution of renewables to the system.

72 The innovative and original contribution of this research study lies in the fact that the proposed  
73 method, with a special focus on islands, is based on the interrelated operation of both the energy  
74 and water sectors. An exploration is undertaken of a significantly large number of new optimal  
75 energy-water infrastructures, determined in all cases on the basis of balanced solutions. The

76 method gives, as a final solution, an optimal water-energy infrastructure with a balance between  
77 energy fuel needs and energy excesses, CO<sub>2</sub> emissions, oil consumption, minimization of total  
78 annual costs and maximization of the renewable contribution. However, after an exhaustive  
79 search of the literature in relation to the renewable water-energy nexus, we detected some gaps  
80 in the current body of knowledge. Therefore, the present research study aims to cover the  
81 following gaps: (i) in previous approaches the water infrastructures remain unaltered and only  
82 strategies based on the energy sector are planned, (ii) consideration is only given to a constant  
83 operating mode in the water supply systems, and no consideration is given to the possibilities  
84 of a variable and interrelated operating mode in the water sector, and (iii) generally, only a  
85 limited number of static energy scenarios are explored. Although the energy planning software  
86 used in this study -EnergyPLAN [19]- is a mature software whose reputation is supported by  
87 more than 349 references in Scopus and 961 results in Google Scholar [20], the work developed  
88 in the present work does not limit its contribution to the application of the EnergyPLAN tool to  
89 the water-energy system of an island, which in itself is an innovation. In fact, a new planning  
90 method is developed, which uses EnergyPLAN but also includes in its procedure an exhaustive  
91 search to generate a large number of feasible alternative optimal scenarios of a target water-  
92 energy system. In addition, the method integrates the Pareto-based multi-objective optimization  
93 concept to facilitate the decision making process of water-energy system planners and  
94 stakeholders. Consequently, no studies were found in the literature survey that could take away  
95 from the novel contributions of the proposed general method. These novel contributions  
96 comprise an approach to optimally manage the variable interrelation of water-energy systems  
97 and a specific method to obtain optimal solutions by varying water and energy infrastructure  
98 designs. The proposed method is applied to Lanzarote, an island in the Canary Archipelago  
99 (Spain) off the northwest coast of Africa.

100 The remainder of the article is structured as follows: Section 2 provides the details of the method  
101 proposed to substantially increase the RES participation in the energy-water system of islands.  
102 In Section 3, the case study used to evaluate the method is introduced. Section 4 provides the  
103 results and a discussion based on the proposed method and case study. Finally, Section 5 shows  
104 the conclusions of the research.

105 **2 Methods**

106 This section describes the basic principles, the tools employed, the approach followed and the  
107 procedures which form the basis of the proposed method to combine the synergies between the  
108 water and energy systems with a view to increasing wind and PV participation in a relatively  
109 small island.

110 **2.1 Basic principles of the method**

111 The Smart Energy Systems concept, first described in 2012 [21] and used for national energy  
112 systems [22], forms the basis for this method. Smart Energy Systems is an approach in which  
113 smart electricity, thermal and gas grids are combined and coordinated to identify synergies  
114 between them with a view to achieving an optimal solution for each individual sector as well  
115 as for the overall energy system. Unlike, for instance, the Smart Grid concept, which puts the  
116 sole focus on the electricity sector, this approach takes into account the entire energy system  
117 along with the identification of suitable energy infrastructure designs and operational strategies  
118 [23]. The method presents certain novelties which make it applicable to water-energy systems  
119 on islands. In this sense, the basic principles which lie behind this new method are as follows:

120 i) The considered approach involves the following energy-water system sectors of the  
121 island: electricity, desalination and wastewater treatment.

122 ii) Due to the inherent fragility of small-sized isolated electric systems (islands), a balanced  
123 energy system configuration, with a lower RES share, will be preferable to an energy

124 system with a higher RES share but which is unbalanced [3]. This determines the way of  
125 choosing the optimum RES configuration for each analysed alternative. To be more  
126 specific, a technical optimization criterion is used based on equaling and minimizing the  
127 sum of the energy surplus (defined as excess electricity production (EEP) [22]) and the  
128 lack of energy when meteorological conditions are insufficient to meet demand with RES.

129 iii) A short-term (hourly) approach in the analysis of the behaviour of intermittent RES (wind  
130 and solar photovoltaic (PV) power) and energy demand is considered. This is done in  
131 order to take into account the fluctuating nature of these energy sources and the potential  
132 for making demand more flexible, in this way adapting it to the intermittent nature of  
133 these RES [3].

134 iv) Higher flexibility in desalination plant operation systems is assumed in relation to the  
135 current way of operation. Studies have been published supporting this technical  
136 possibility [14,24], allowing the exploration of new scenarios in which, for instance,  
137 desalination capacity can be oversized with respect to water demand, attending to  
138 sustainable techno-economic criteria. So, for example, desalination plants can be  
139 managed to satisfy water demand and, when RES are fully available, to generate a surplus  
140 amount of fresh water which can then be stored or, when the RES are in short supply, to  
141 reduce production.

142 v) The proposed method is designed for islands, which implies a renewable desalination  
143 infrastructure search based not only on water demand criteria but also on obtaining a  
144 balanced energy system configuration.

## 145 2.2 EnergyPLAN simulation tool

146 Various models are available to analyse the contribution of renewables in energy systems [25].  
147 However, certain characteristics of EnergyPLAN which are closely related to the basic

148 principles on which this research is based (section 2.1) make it an ideal tool for this study. For  
149 example, EnergyPlan allows the empirical modelling of an energy system and performs hourly  
150 simulations with a time frame of one year [26]. In addition, it was designed specifically to apply  
151 the Smart Energy System concept and is capable of simulating the entire energy system and  
152 interrelate the different sectors. Descriptions of the algorithm can be consulted in the different  
153 manuals, reports and documents published on the website [www.energyplan.eu](http://www.energyplan.eu). EnergyPLAN  
154 is capable of considering desalination as a flexible electricity demand and, hence, is able to  
155 manage its operation in a smart way to allow the integration of more renewables. However,  
156 desalination can also be considered inflexible, and this can also be exploited to determine  
157 whether increasing flexibility in the water sector can be used to increase renewable participation  
158 in an energy system. Another important feature of EnergyPLAN of interest for this study is its  
159 relatively fast capacity to model and simulate each new scenario. The approach presented in  
160 this research requires a huge number of simulations to find the optimal scenarios and, hence,  
161 computing time is a factor that needs to be taken into account.

162 **2.3 The MATLAB Toolbox for EnergyPLAN designed to automate the analysis of a  
163 large number of new alternative scenarios**

164 Although EnergyPLAN has a user-friendly interface, it only allows the user to run a limited  
165 number of subsequent executions, varying a limited number of decision variables for a concrete  
166 modelled energy system [20]. This manual mode, in which EnergyPLAN combines the  
167 optimization of both the operational phase and the planning phase, has been mentioned by other  
168 authors [27–29]. To explore new benefits of the tool, many have realized the need to combine  
169 EnergyPLAN with other computational tools [28–30]. The MATLAB Toolbox for  
170 EnergyPLAN was developed in this context, comprising a set of functions wrapped in a toolbox  
171 designed to call and manage EnergyPLAN from MATLAB [20]. In this study, this toolbox  
172 plays an essential role by allowing the automated generation of a large number of new

173 alternative scenarios from MATLAB. Additionally, the huge set of results can be analysed  
174 using big data techniques available in MATLAB.

175 **2.4 Multi-objective optimization model**

176 In this study, a Pareto-based multi-objective optimization model is applied. This model allows  
177 the calculation of a set of acceptable trade-off possible optimal solutions, called Pareto front  
178 [29–35]. These solutions are obtained on the basis of all the different conflicting objectives  
179 chosen for the evaluated water-energy system [32]. This resulting Pareto front allows the  
180 decision makers a better understanding of the overall system, enabling them to explore all the  
181 consequences of a decision with respect to the various conflicting objectives [32,36].

182 According to [37–39], a multi-objective problem can generally be formulated as follows:

$$\begin{aligned} & \text{minimize:} & \mathbf{y} = \mathbf{f}(\mathbf{x}) = (f_1(\mathbf{x}), f_2(\mathbf{x}), \dots, f_k(\mathbf{x})) \\ & \text{subject to:} & \begin{cases} \mathbf{g}(\mathbf{x}) = (g_1(\mathbf{x}), g_2(\mathbf{x}), \dots, g_m(\mathbf{x})) \leq \mathbf{0} \\ \mathbf{h}(\mathbf{x}) = (h_1(\mathbf{x}), h_2(\mathbf{x}), \dots, h_p(\mathbf{x})) = \mathbf{0} \\ l_i \leq x_i \leq u_i, \quad i = 1, 2, \dots, n \end{cases} \\ & \text{where:} & \begin{cases} \mathbf{x} = (x_1, x_2, \dots, x_n) \in \mathbf{X} \\ \mathbf{y} = (y_1, y_2, \dots, y_k) \in \mathbf{Y} \end{cases} \end{aligned} \tag{1}$$

183  $\mathbf{x}$  is the vector of  $n$  decision variables (parameters) and  $\mathbf{y}$  is the vector of  $k$  objective functions.  
184  $\mathbf{X}$  is denoted as the decision space and  $\mathbf{Y}$  is called the objective space.  $\mathbf{g}(\mathbf{x})$  is a set of  $m$   
185 inequality constraints with feasible solutions ( $\mathbf{e}(\mathbf{x}) \leq \mathbf{0}$ ), and  $\mathbf{h}(\mathbf{x})$  represents a set of  $p$   
186 equality constraints.  $l_i$  and  $u_i$  are used to represent the lower and upper limits of the  $i$ -th  
187 variable, respectively.

188 To compare candidate solutions to the multi-objective problem, the concepts of feasible  
189 solution, feasible solution set, Pareto dominance, Pareto optimal solution, Pareto optimal set  
190 and Pareto front are introduced [39]:

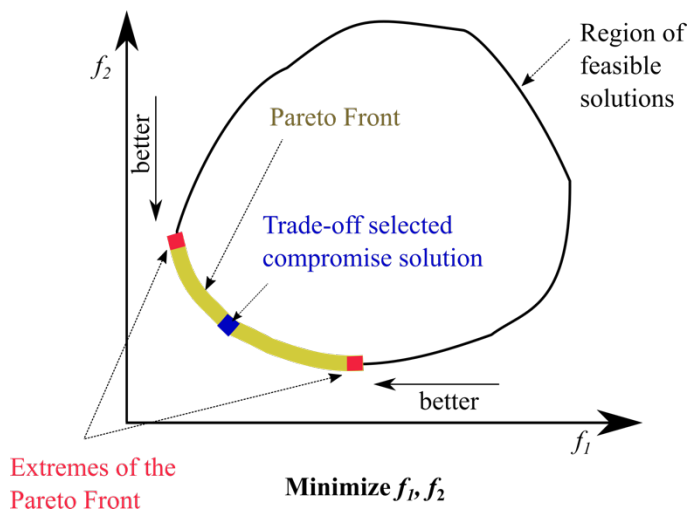
191 If a candidate solution  $\mathbf{x} \in \mathbf{X}$  satisfies the constraints in Eq.(1), then  $\mathbf{x}$  is called a *feasible*  
192 *solution*. All feasible solutions conform the *feasible solution set*.

193 Formally, it is said that a feasible solution  $x$  Pareto dominates another feasible solution  $x'$  if  
194 and only if:

$$\begin{cases} f_i(\mathbf{x}) \leq f_i(\mathbf{x}'), & \forall i \in \{1, 2, \dots, m\} \\ f_i(\mathbf{x}) < f_i(\mathbf{x}'), & \exists i \in \{1, 2, \dots, m\} \end{cases} \quad (2)$$

195 Therefore,  $x$  is called a *Pareto optimal solution*, or Pareto non-dominated solution, if and only  
196 if it is not dominated by any other feasible solution. This means that solution  $x$  cannot be  
197 improved in one of the objectives without adversely affecting another objective [36]. The set  
198 of all Pareto optimal solutions is called the *Pareto optimal set* and the corresponding objective  
199 vectors are said to be on the Pareto front (Fig. 1). The analytical expression of the Pareto front  
200 cannot usually be obtained in practical problems [36,39].

201 Fig. 1 represents the Pareto front of a two-objective minimization problem.



20

**Fig. 1.** Representation of the Pareto front for a two-objective minimization problem. Adapted from [36,39].

204

205 The solutions above the yellow line have at least one objective function inferior to that of  
 206 another solution not included in the Pareto front [32]. The selection of solutions situated in the

207 extremes of Pareto fronts (plotted in red in Fig. 1) guarantees the best performance for one  
 208 objective function criterion but an improveable performance for the others. Conversely, a more  
 209 centered solution within the Pareto front (trade-off solution plotted in blue in Fig. 1) guarantees  
 210 a balance between different objective functions criteria which allows a better overall  
 211 performance of the system attending to different parameters. This trade-off analysis is critical  
 212 in the decision making process of energy system planners and stakeholders [40]. The method  
 213 to select this trade-off compromise solution is described in section 2.5.5.

214 The particular application of the optimization model to the water-energy systems on islands can  
 215 be represented as follows:

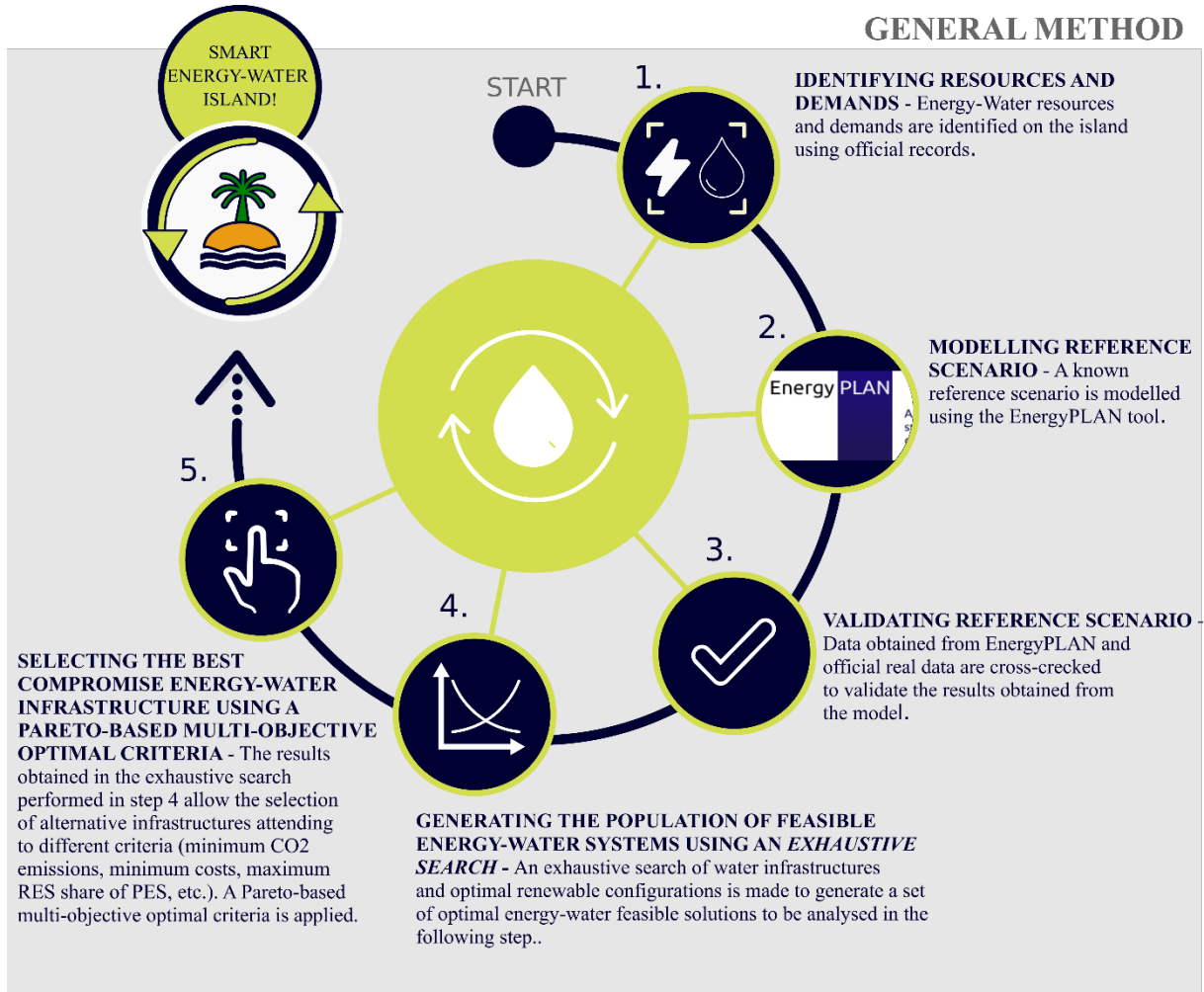
$$\begin{aligned}
 \text{minimize:} \quad & y_1 = \text{total annual } CO_2 \text{ emissions (Mt)}, \\
 & y_2 = 100\% - \text{RES share of PES (\%)}, \\
 & y_3 = \text{total annual fuel consumption, PES, (TWh)}, \\
 & y_4 = \text{total annual oil contribution to PES (TWh)}, \\
 & y_5 = \text{maximum required hourly import (MW)}, \\
 & y_6 = \text{imports/exports intersection point (TWh)}, \\
 & y_7 = \text{annual variable costs (M\text{\euro})}, \\
 & y_8 = \text{total annual costs (M\text{\euro})}, \\
 \\ 
 \text{subject to:} \quad & \text{Current water storage capacity} \leq x_1 \leq \text{maximum feasible value}, \\
 & \text{Current desalination capacity} \leq x_2 \leq \text{maximum feasible value}, \\
 & \text{Current wind power} \leq x_3 \leq \text{wind power to cover 100\% electr. demand}, \\
 & \text{Current PV power} \leq x_4 \leq \text{PV to cover 100\% electricity demand}, \\
 \\ 
 \text{where:} \quad & x_1 = \text{water storage capacity (Mm}^3\text{)}, \\
 & x_2 = \text{desalinated water production capacity (1000 m}^3\text{/h}), \\
 & x_3 = \text{wind power installed capacity (MW)} \\
 & x_4 = \text{PV power installed capacity (MW)},
 \end{aligned} \tag{3}$$

216 This problem is generally formulated by 4 decision variables (water storage capacity,  
 217 desalination water capacity, wind power capacity installed in the energy system and PV power  
 218 capacity) and 8 potential objective functions. However, the number of potential objective

219 functions can be increased or reduced depending on data availability or the aims of the decision  
220 makers. The potential objective functions are the annual CO<sub>2</sub> emissions, the RES share of PES,  
221 the total annual fuel consumption (PES), the total annual oil contribution to PES, the maximum  
222 required hourly import, the intersection point of imports and exports for each water  
223 infrastructure (which defines the energy storage size required to minimize fossil fuel  
224 consumption), the annual variable costs, and the total annual costs. All of these objective  
225 functions are calculated by the EnergyPLAN software. Their mathematical model and detailed  
226 descriptions can be found in [19,41].

227 **2.5 Detailed description of the procedure**

228 The different steps of the method used in this research are shown in Fig. 2. The procedure can  
229 be applied to any island in the world for future studies with similar objectives.



230  
231  
232

**Fig. 2.** Graphical step-by-step representation of the general method.

233 **2.5.1 Step 1. Identification of the energy-water resources and demands**  
 234 First, the current energy-water resources and demands on the target island are identified. The  
 235 data collected in this step are available in official reports and statistics published by local  
 236 institutions and governments [42–46]. Additionally, in this first step, it is recommended to map  
 237 the potential viable growth of the different resources that are available, the potential installation  
 238 and use of new resources, any particular features of the target island that could benefit or limit  
 239 the future exploitation of RES, and any existing medium- or long-term energy plans.

240 2.5.2 *Step 2. Reference scenario modelling*

241 In the second step, the EnergyPLAN freeware is used to model a known reference scenario of  
242 the target island. This basically involves introducing all energy-water data and hourly  
243 distributions into the software and making initial simulations. After this model has been  
244 validated, which is carried out in the third step of the approach, alternative scenarios can then  
245 be realistically simulated using EnergyPLAN.

246 2.5.3 *Step 3. Reference scenario validation*

247 The validation carried out in the third step consists of cross-checking the results obtained from  
248 the EnergyPLAN model and the known real data. This allows a quantification of the deviation  
249 between model and reality with the aim of knowing the error in the simulation and presenting  
250 the results in a rigorous way.

251 2.5.4 *Step 4. Generation of the population of  $n$  alternative feasible optimal solutions using  
252 an exhaustive search*

253 The fourth step is the most complex part of the method and is supported by the MATLAB  
254 Toolbox for EnergyPLAN [20]. In this step of the process an iterative and layered approach is  
255 developed to find the optimal RES configuration for each new alternative water infrastructure.  
256 As can be seen in Fig. 3, the MATLAB Toolbox for EnergyPLAN [20] plays a key role in  
257 receiving the reference scenario previously validated in EnergyPLAN. The variables which  
258 define this reference scenario are divided into two groups: unaltered variables and alterable  
259 variables. While the first ones are not changed when new alternative scenarios are built, the  
260 alterable variables are modified in an iterative way with the aim of generating the population  
261 of optimal solutions, as can be seen in detail in Fig. 4. This search procedure considers the  
262 basic principles set out in section 2.1 and is performed as follows:

263 i) New scenarios are created modifying one of the alterable decision variables related to the  
264 water infrastructure. Both the water production and storage capacities on the island are  
265 modified in a nested way. For each variation in water storage capacity, water production  
266 capacity is modified step by step within a viable range previously calculated for the target  
267 island.

268 ii) For each new scenario, the alterable variables related to installed RES power are changed.  
269 A search is made for a new balanced RES configuration for each new alternative water  
270 infrastructure. This search is based on the technical optimization criterion proposed by  
271 Cabrera et al. in [3]. The procedure equalizes and minimizes the sum of the hourly energy  
272 surpluses and the energy shortages when meteorological conditions are insufficient to meet  
273 demand with RES [3]. When wind and PV power capacities increase, the possibility of an  
274 electricity surplus also increases. This energy surplus (or Export in this study) is defined  
275 as the EEP [22]. A fossil fuel energy need (or Import) occurs when wind and solar  
276 conditions are insufficient to meet demand, assuming power plant generation is to be  
277 completely avoided [3]. The minimum intersection point of imports and exports was  
278 obtained for each water infrastructure. In this study, ‘Imports’ are the hourly electrical  
279 needs that renewable sources are unable to satisfy, and ‘Exports’ corresponds to the hourly  
280 electric renewable generation which the system is unable to use because the demand at the  
281 moment of production is insufficient to match it. While Imports and Exports are equal and  
282 null in ideal balanced energy systems, the optimal configuration is considered to be that  
283 which obtains import/export values that are equal and as close to zero as possible [3]. To  
284 find this configuration, each water infrastructure was executed 100 times (as the renewable  
285 power capacities of both wind and PV are varied 10 times each in an iterative and sequential  
286 loop). With the aim of ensuring the stability and security of the electrical power system, an  
287 extra generation of electrical energy was considered in each water infrastructure. Since this

288 study was undertaken from an energy planning point of view, the possible reconfiguration  
 289 of the electric grid —and other problems derived from the massive RES increase in the  
 290 grid— was not analysed. In this respect, previous studies [3,47] suggest that the use of  
 291 currently available equipment such as synchronous compensators (SCs) can provide active  
 292 power [3,47] and serve the needs of all ancillary services of conventional generators except  
 293 those requiring reactive power (fault current, inertia and voltage support) [47]. The  
 294 configuration which obtained the minimum intersection point was then analysed in more  
 295 detail, using the same hourly distribution profiles as in the 2018 reference scenario. This  
 296 method allows measurement of the PES by fuel type to assess the impact on the energy  
 297 mix [22], on total annual CO<sub>2</sub> emissions [22], and on other variables such as the minimum  
 298 export required in each scenario, the variable and total annual costs, and the required wind  
 299 and PV power capacities (Fig. 3).

300 iii) In this way, an optimal balanced RES scenario for each water infrastructure proposal is  
 301 obtained. Each optimal configuration is defined by eight key variables, as shown in Fig. 3.

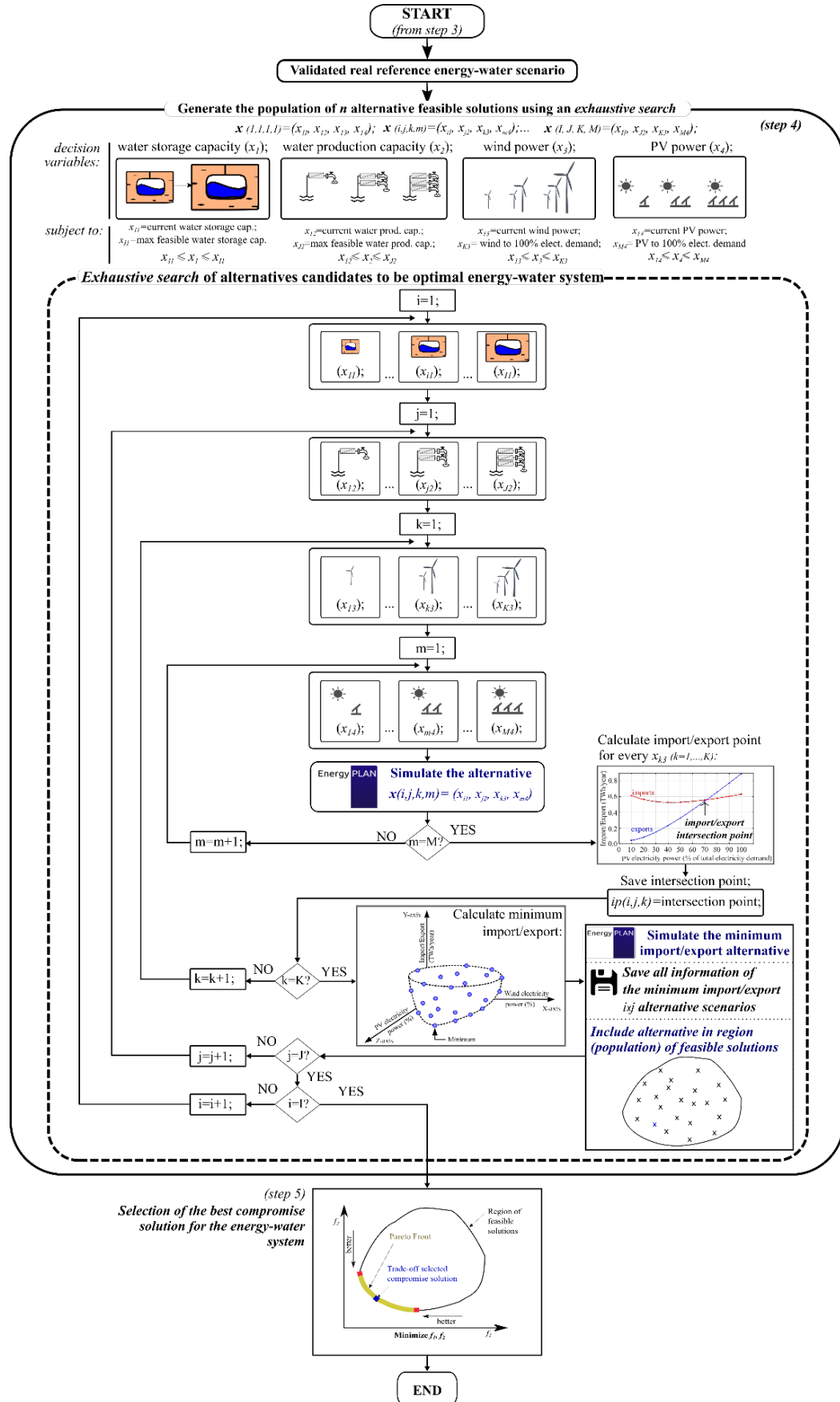
302



304 **Fig. 3.** Software framework and global outline to generate the population of optimal energy-water infrastructures  
 305 executed in step 4 of the general method.

306

307 The search method designed and carried out in this step is described in greater detail in Figure  
308 4. It is presented in the form of a block diagram to make it easier to understand and reproduce.  
309 The method begins with the model validated from the reference scenario used in the study  
310 (constructed in the previous steps: 1, 2 and 3). On the basis of this model, at the start of the  
311 procedure the decision variables are defined:  $x_1$  = water storage capacity;  $x_2$  = water production  
312 capacity;  $x_3$  = installed wind power;  $x_4$  = installed PV power. The values are defined following  
313 the constraints established for these variables, so that the search method does not exceed the  
314 limits imposed for each of them. Subsequently, the *exhaustive search* is initiated to create the  
315 feasible optimal solution set. This procedure is carried out in a robust way, through a series of  
316 nested loops which explore all the possible values defined for the decision variables. Firstly,  
317 for each value of water storage capacity ( $x_1$ ), water production capacity ( $x_2$ ) and installed wind  
318 power ( $x_3$ ), all the values defined for installed PV power ( $x_4$ ) are run. As previously commented,  
319 in this study it was determined to increase this decision variable 10 times, from its initial value  
320 (current installed PV power) to its final value (installed PV power to cover 100% of the  
321 electricity demand in the system).



325 With each variation of the decision variables a simulation is executed of the new alternative  
326 scenario derived from the initial validated reference scenario. From each of these simulations,  
327 the pairs of results in *imports* and *exports*<sup>2</sup> which provide these alternative solutions are stored.  
328 Once all the values defined for  $x_4$  have been run, the curves of *imports and exports* are plotted  
329 and their intersection point is calculated. The result is also stored of this intersection point  
330 obtained for the alternative analysed; for this the vector  $ip(i,j,k)$  is used. When this procedure is  
331 concluded, the index  $k$  is increased by a value to analyse the following set of scenarios with a  
332 new value of  $x_3$ . So, the search is repeated of the new intersection point of *imports and exports*  
333 for the new value  $x_3$ . As described, the variation of  $x_3$  was considered similar to that of  $x_4$ . This  
334 decision variable ( $x_3$ ) is also increased 10 times, from its initial value (current installed wind  
335 power) to its final value (installed wind power to cover 100% of the electricity demand in the  
336 system). When the procedure finishes running all the possible values of  $x_3$ , a new three-  
337 dimensional representation is constructed which represents the previously calculated  
338 intersection points on the Y-axis for the corresponding values of the other decision variables  
339 involved, installed wind power on the X-axis and installed PV power on the Z-axis. With this  
340 three-dimensional representation, the minimum value of the import/export intersection point is  
341 calculated. In this way, the sum of the hourly energy surpluses and the energy shortages is  
342 equalised and minimised in accordance with the basic principle ii) of the method (section 2.1).  
343 This alternative scenario is again simulated with EnergyPLAN and all the information obtained  
344 from that simulation is stored (CO<sub>2</sub> emissions, RES share of the primary energy supply (PES),  
345 total annual PES, total annual oil contribution to PES, maximum power necessary from  
346 conventional sources (maximum import), import/export intersection value, variable costs, total  
347 annual costs, etc.). This alternative scenario is likewise included in the set of feasible optimal  
348 solutions that will be explored later (in step 5). In this way, it is possible to have all the

---

<sup>2</sup> The meaning of the variables *import* and *export* is described in point ii) of section 2.5.4.

349 information necessary for the multi-objective optimization that is proposed for the global  
 350 method. Finally, the procedure indicated is repeated for each of the values of  $x_2$  and  $x_1$  defined  
 351 at the start, varying the indices  $j$  and  $i$ , respectively.

352 *2.5.5 Step 5. Selection of the best compromise solution for the energy-water system*

353 The most important decision variables are obtained for each optimal configuration and, hence,  
 354 in this step a Pareto-based multi-objective optimal criteria is applied. More specifically, an  
 355 optimal energy-water configuration is reached based on a trade-off of the following criteria:  
 356 CO<sub>2</sub> emissions, RES share of the PES, total annual PES, total annual oil contribution to PES,  
 357 maximum power necessary from conventional sources (maximum import), import/export  
 358 intersection value, variable costs and total annual costs. To find this best compromise solution,  
 359 the following approach is proposed [48]. Mathematically, the  $i$ -th objective function  $\mathbf{y}_i$  is  
 360 represented by a membership function  $\mu_i$  defined by Eq. (3) [48]:

$$\mu_i = \begin{cases} 1 & y_i \leq y_i^{\min} \\ \frac{y_i^{\max} - y_i}{y_i^{\max} - y_i^{\min}} & y_i^{\min} < y_i < y_i^{\max} \\ 0 & y_i \geq y_i^{\max} \end{cases} \quad (3)$$

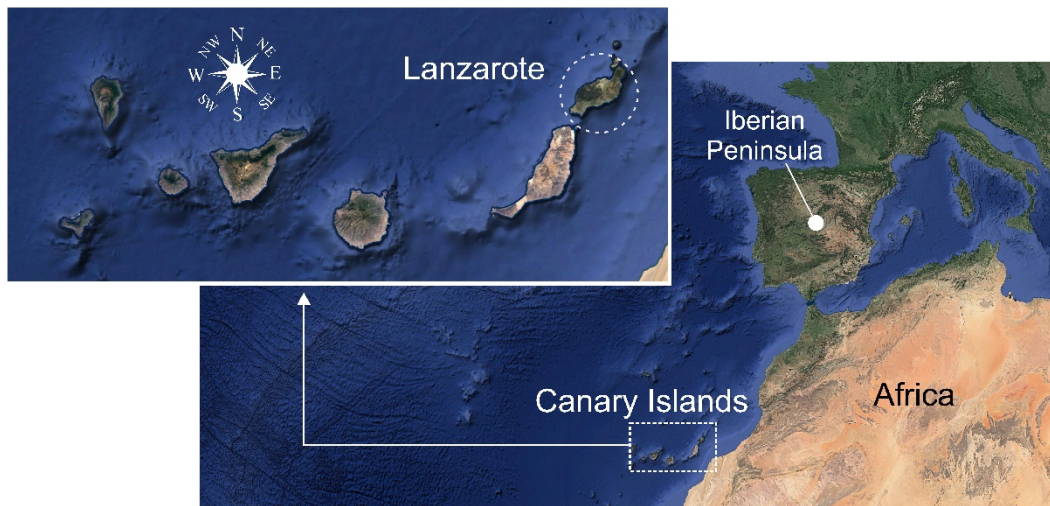
361 where  $y_i^{\min}$  and  $y_i^{\max}$  are the minimum and maximum value of the  $i$ -th objective function  
 362 among all non-dominated solutions (situated in the Pareto front), respectively. For each non-  
 363 dominated solution  $k$ , the normalized membership function  $\mu_i^k$  is calculated as:

$$\mu_i^k = \frac{\sum_{i=1}^{N_{obj}} \mu_i^k}{\sum_{k=1}^M \sum_{i=1}^{N_{obj}} \mu_i^k} \quad (4)$$

364 where  $M$  is the number of non-dominated solutions. The best compromise solution is the one  
 365 with the maximum value of  $\mu_i^k$ .

366 **3 Case study: application of the method in the island of Lanzarote**

367 Lanzarote is a Spanish island located in the Atlantic Ocean about 125 km off the north coast of  
368 Africa and 1,000 km from the Iberian Peninsula [49] (Fig. 5). At the start of 2019, Lanzarote  
369 had a population of 152,289 inhabitants [43].



370  
371 **Fig. 5.** Geographical location of the island of Lanzarote. [Source of satellite images: Google Earth: ©2020 Data  
372 SIO, NOAA, U.S. Navy, NGA, GEBCO, Landsat/Copernicus, IBCAO ©2020 GRAFCAN].  
373

374 **3.1 Identification of energy-water resources and demands**

375 Firstly, the current energy-water resources and demands of Lanzarote were mapped.  
376 Additionally, as suggested in section 2.5, the specific particularities of the island were identified  
377 along with the energy-water plans and regulations.

378 **3.1.1 The energy system in Lanzarote**

379 Based on the official energy reports published by the Canary Islands Regional Government  
380 [42], the energy system of Lanzarote can be represented by the Sankey diagram shown in Fig.  
381 6. With more than 94.5% of the total PES system based on oil (fundamentally fuel oil, gasoil  
382 and gasoline), Lanzarote has a very high dependence on fossil fuels [42]. In 2018, installed  
383 wind and solar energy only contributed 5.14% of the energy needs of the island. Finally, natural  
384 gas was used to satisfy around 2.9% of the energy requirements. It can be seen in Fig. 6 that the  
385 highest amount of fuels were used to feed the power plants responsible for generating electricity

386 (2175.7 GWh). The transport sector also consumed an important quantity of energy, (1084 and  
387 71 GWh in road and maritime transport, respectively). From the total energy required to feed  
388 the power plants (2175.7 GWh), only 854 GWh were generated in the form of electricity which,  
389 when added to the 50.96 GWh supplied by wind and the 9.50 GWh by solar PV, satisfied the  
390 total electricity demand of 914.46 GWh. Almost 59% of this generation (539.5 GWh) supplied  
391 a considerable part of the energy needs of the services, industry and construction sector (with a  
392 total energy demand of around 724.3 GWh). The heating and cooling data were not obtained  
393 directly from official reports but were estimated from different consumption statistics and  
394 energy audit reports drawn up by consumer groups and the Canary Regional Government  
395 [45,50]. As a consequence of the above, and the fact that the authors of the present study were  
396 unable to find any study that had analysed the heating and cooling demand on the island, it was  
397 decided to exclude these data from the analysis undertaken in the present study. Nonetheless,  
398 preliminary analyses suggest promising results in terms of increasing renewable integration if  
399 new similar studies were able to focus on these sectors and/or the transport sector on the basis  
400 of reliable data and statistical analyses. With the currently available data, we estimated heating  
401 and cooling demands of approximately 187 and 89.5 GWh. Both are mostly consumed by  
402 hotels, commerce and the service sector. More oriented to the particular aim of this research,  
403 the desalination sector is entirely powered by electricity and required a total of 91 GWh, which  
404 is around 10% of total electricity demand [51,52].

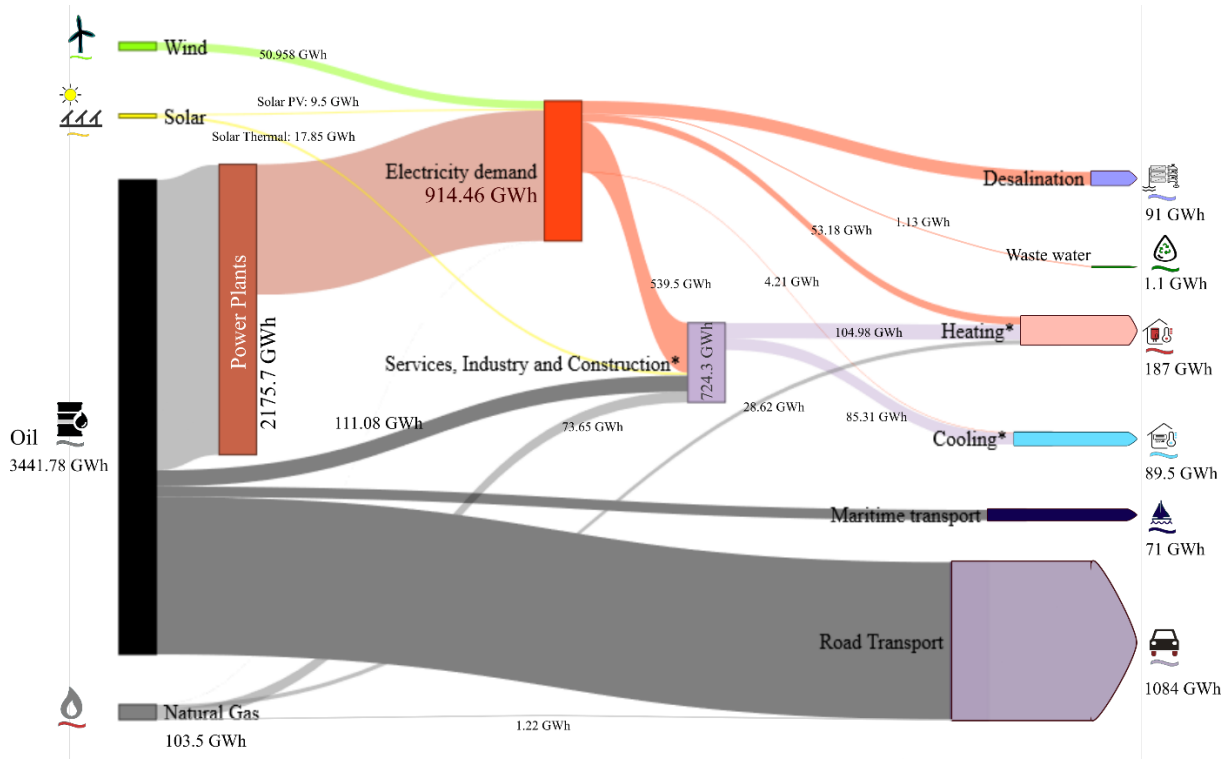


Fig. 6. Sankey diagram of the Lanzarote 2018 energy system. Data sources: [42,43,52,53].

\*These energy values are not measured but estimated from statistical data and reports.

405  
406  
407  
408

409 After analysing the whole energy system of Lanzarote and the Sankey diagram represented in  
410 Fig. 6, it is possible to infer the following interpretations with respect to the target objective of  
411 this research:

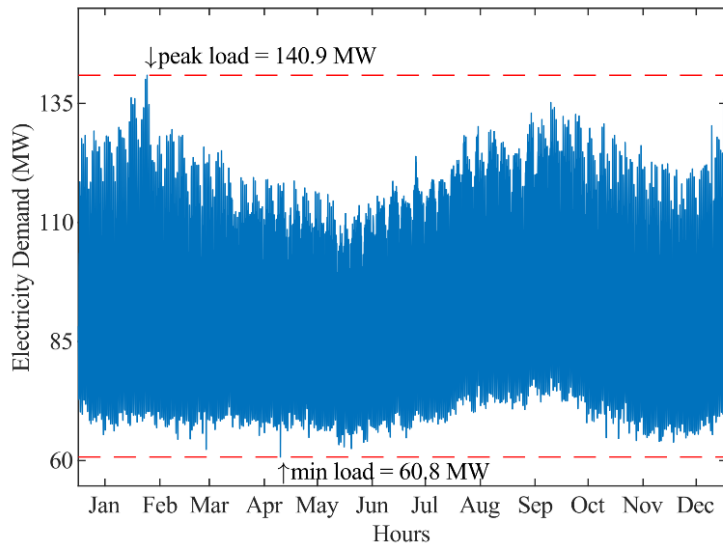
412 a) Electricity is the main energy use on Lanzarote  
413 b) Desalination is not the biggest demand on the island. However, it represents an important  
414 electrical energy consumption and can be managed as a flexible demand with some  
415 relatively easy innovations [3,10,14]

416 c) The participation of renewables in the current energy system is very low

417 In the following subsections, we therefore focus on the electricity and desalination systems with  
418 the aim of identifying the corresponding demand and resources.

419 3.1.2 *Electricity demand and potential electrical resources in Lanzarote*

420 The electricity demand in Lanzarote shows a peak load at the end of January (around 141 MW)  
421 and a minimum load in April (60.8 MW) (Fig. 7). This behavior is highly conditioned by the  
422 seasonal nature of tourism on the island. Lanzarote usually welcomes a significant number of  
423 tourists in this period [53].

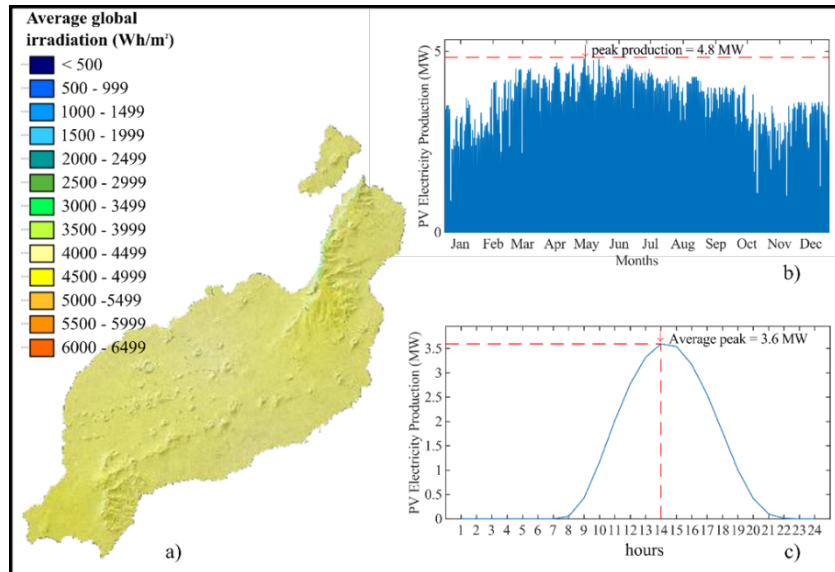


424  
425 **Fig. 7.** Hourly average electricity demand in Lanzarote, 2018 [54].

426 Currently, Lanzarote has 13 generators (11 diesel and 2 gas-based) with a total net power  
427 capacity of 204.82 MW [46]. The island is electrically connected via a submarine cable to its  
428 neighbouring island, Fuerteventura, which has 159.27 MW of installed power.

429 Despite the relatively high available sun and wind energy resource in Lanzarote (see Fig. 8a  
430 and Fig. 9a, respectively), the current renewable installed power is low. In 2018, the islands had  
431 9 MW installed PV capacity and 22.3 MW installed wind power capacity [46]. Peak PV  
432 production in 2018 was only 4.8 MW (Fig. 8b), and the average hourly peak production of 3.6  
433 MW was produced at 14:00 h (Fig. 8c).

434

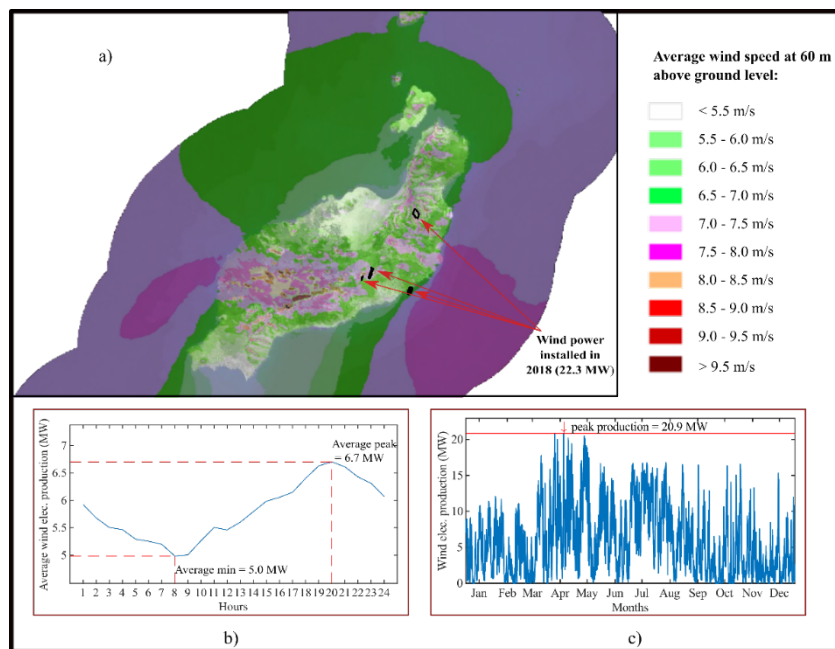


435

436 **Fig. 8.** Photovoltaic energy resource in Lanzarote. a) Average global irradiation map for the island of Lanzarote;  
 437 b) Mean hourly PV electricity production in Lanzarote, 2018; c) Daily pattern of mean hourly PV electrical  
 438 power production in Lanzarote, 2018. Source of maps: [55]; Source of electrical power production data: [54].

439

440 With only 22.3 MW of installed wind power (Fig. 9a), peak production was at the end of April  
 441 when a value of 20.9 MW was recorded (Fig. 9c). Peak hourly production averaged 6.7 MW  
 442 and happened around 20:00 h, while the corresponding minimum value was 5.0 MW at around  
 443 08:00 h (Fig. 9b).



444

445 **Fig. 9.** Wind energy resource in Lanzarote. a) Average wind speed map for the island of Lanzarote; b) Daily  
 446 pattern of mean hourly wind power production in Lanzarote, 2018; c) Mean hourly wind electricity production in  
 447 Lanzarote, 2018. Source of maps: [55]; Source of electrical power production data: [54].

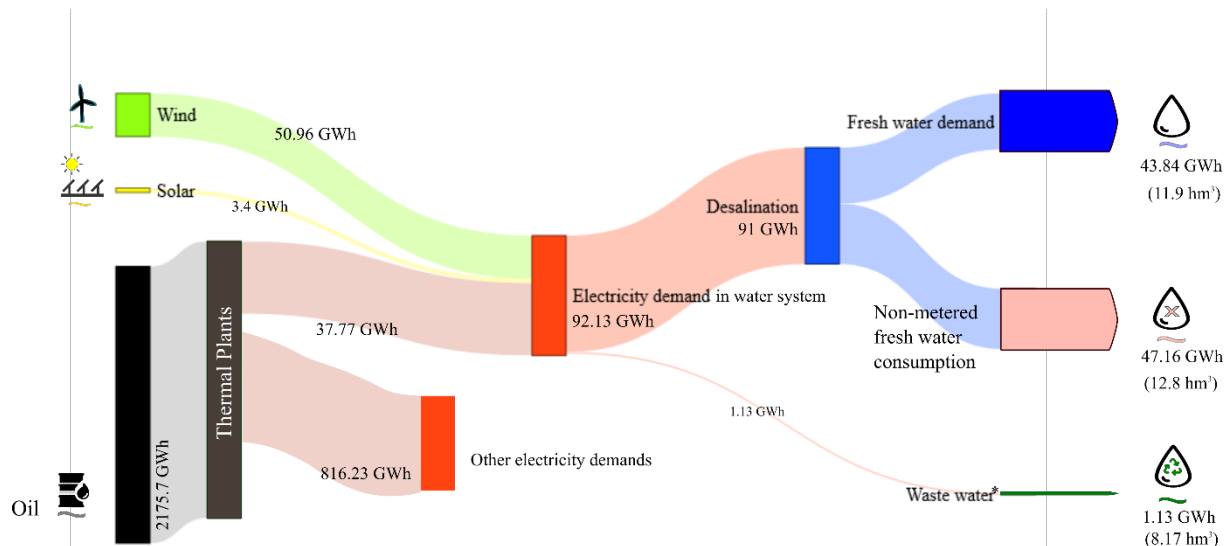
448 3.1.3 Water sector in Lanzarote

449 The resources, needs and particularities of the Lanzarote water system are described below.

450 3.1.3.1 Energy demand in the water sector

451 Fig. 10 represents the energy resources and needs associated to the 2018 Lanzarote water sector.

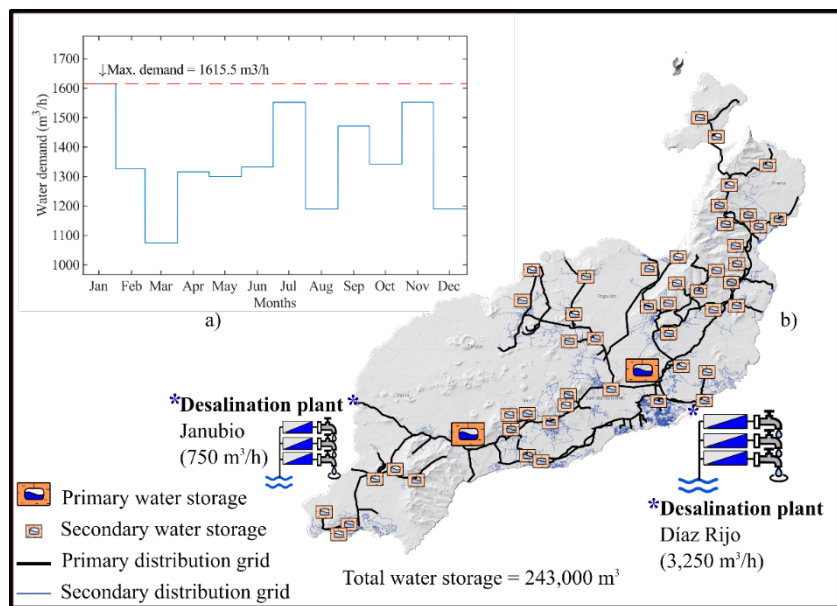
452 As can be seen, the total amount of wind energy (50.96 GWh) satisfies part of the annual  
 453 desalination electricity demand (91 GWh). Solar PV energy also contributes 3.4 GWh to  
 454 desalination. The wind and PV power facilities which supplied these amounts of energy were  
 455 installed by the Lanzarote Water Board with the aim of promoting desalination with renewables  
 456 [56]. As can be seen, in the current water system in Lanzarote there is greater non-metered than  
 457 metered freshwater consumption. According to the current operating company of the water  
 458 sector (Canal Gestión Lanzarote S.L.), this is largely due to water leaks in the old distribution  
 459 grid of Lanzarote [57,58].



460  
 461  
 462 **Fig. 10.** Sankey diagram of the energy flow in 2018 Lanzarote water system. Data sources: [46,51,53,59,60]  
 463 \*These energy values are not measured but estimated from specific energy consumptions calculated by previous  
 464 studies in the area [61].  
 465

466        3.1.3.2 *Water production and distribution*

467        Fig. 11 shows the water production system in Lanzarote. Water demand on the island is entirely  
 468        dependent on RO desalination centers installed on the west and east coasts. As can be seen,  
 469        Lanzarote has an interconnected water distribution grid based on a large number of small water  
 470        storage tanks and two larger ones situated in the center and south of the island (Fig. 11b)  
 471        [51,53,62]. Total water storage capacity is around 243,000 m<sup>3</sup>. Water demand presents three  
 472        peaks, two in winter (period with more tourist visits) and one in summer (period with most  
 473        water needs) (Fig. 11a).



474        **Fig. 11.** Water system in Lanzarote. a) Water demand in the island of Lanzarote; b) Water distribution grid in  
 475        Lanzarote. Source of data: [51,53,59].

477

478        3.1.3.3 *Water reuse*

479        Although the island does have a water reuse infrastructure [56], not all water production is  
 480        reused (8.17 hm<sup>3</sup> of the total 24.7 hm<sup>3</sup> of freshwater produced) and only a small amount of this  
 481        reused water passes through a tertiary treatment (2.9 hm<sup>3</sup>) to prepare the water for reuse in  
 482        profitable applications such as irrigation in the agriculture sector. This water infrastructure  
 483        appears to be a potential candidate for development in terms of increasing efficiency and the

484 renewable contribution to the system. In this respect, it should be noted that an appropriate  
485 water reuse system not only could be powered by RES, but could also help to minimize part of  
486 the current energy supplied to produce freshwater. However, the difficulty in obtaining accurate  
487 and reliable statistical data related to this water use means that a more specific study is required  
488 to analyse this topic.

489 **3.2 Cost assumptions for the modelling of the reference scenario in EnergyPLAN**

490 In this step, the reference scenario was modelled in EnergyPLAN after introducing all the  
491 identified data in the tool. The cost assumptions considered in this study are based on different  
492 real data and assumptions calculated by different institutions, including the Danish Energy  
493 Agency [63], the Spanish Institute for Diversification and Energy Saving [64], and other local  
494 organizations [46,52,53,65]. The most relevant costs are presented in Table 1. The cost  
495 assumptions are total investments before discounts. The fixed operation and maintenance costs  
496 are estimated as a percentage of investment costs.

497 **Table 1:** Costs of the most important installations considered in the study.

Installation	Investment cost	Fixed O&M (%)	Lifetime (years)
Power plants	0.99 M EUR/MW-e	3.05	20
Wind power	1.2 M EUR/MW-e	2.97	20
Photovoltaic	0.5 M EUR/MW-e	0.6	20
Desalination plants	1000 EUR/m <sup>3</sup> fresh water	3	20
Water storage	113.33 EUR/m <sup>3</sup>	1	20

498  
499 Additionally, a CO<sub>2</sub> price of 24.92 EUR/t CO<sub>2</sub> is considered based on the historical data of this  
500 value for the EU [66]. The most important fuel costs considered are presented in Table 2.

501 **Table 2:** Fuel costs considered in the study.

Fuel	Price (EUR/GJ)
Diesel	15
Fuel oil	11.9
Natural gas	9.1

502

503 **3.3 Validation of the reference scenario modelled in EnergyPLAN**

504 After identifying the energy system and modelling the reference scenario in EnergyPLAN, the  
 505 operating simulation which EnergyPLAN performs was validated. As shown in Table 3, Table  
 506 4, Fig. 12, Fig. 13, Table 5 and Table 6, a comparison was made between the results of the 2018  
 507 Lanzarote energy system and the simulation performed by EnergyPLAN at a 1-h time  
 508 resolution. The monthly energy electricity demands obtained from EnergyPLAN and from the  
 509 actual data gathered from official data reports are compared in Table 3. The comparison of peak  
 510 electricity powers supplied is shown in Table 4, the difference between the electricity produced  
 511 from various units in actual data and simulations in Table 5, and annual fuel consumption by  
 512 energy source in Table 6.

513 **Table 3:** Average monthly electricity demand obtained from the EnergyPLAN model and actual values for the  
 514 year 2018 in Lanzarote.

Month	Actual 2018 (GWh)	EnergyPLAN 2018 (GWh)	Difference (GWh)	Difference (%)
January	72.98	75.03	2.05	2.81
February	66.70	66.46	-0.24	-0.36
March	71.13	69.83	-1.30	-1.83
April	68.06	67.51	-0.56	-0.82
May	69.03	68.49	-0.55	-0.79
June	67.47	66.74	-0.73	-1.09
July	72.30	73.37	1.07	1.48
August	76.31	73.96	-2.35	-3.08
September	74.62	74.51	-0.10	-0.14
October	75.03	75.37	0.34	0.45
November	68.83	70.50	1.66	2.42
December	72.61	72.28	-0.33	-0.46
<b>Total</b>	<b>855.08</b>	<b>854.05</b>	<b>-1.04</b>	<b>-0.12</b>

515  
 516 Table 3 shows that the maximum absolute differences obtained between the modelled monthly  
 517 electricity energy demands and their actual values are produced in August (2.35 GWh), January  
 518 (2.05 GWh) and November (1.66 GWh), respectively. These values are relatively low if their  
 519 relative percentages are considered (all differences present relative values below 3.5%). These  
 520 small differences in energy demands are produced because in the real data the power  
 521 consumption for water systems is integrated into the overall power consumption of the

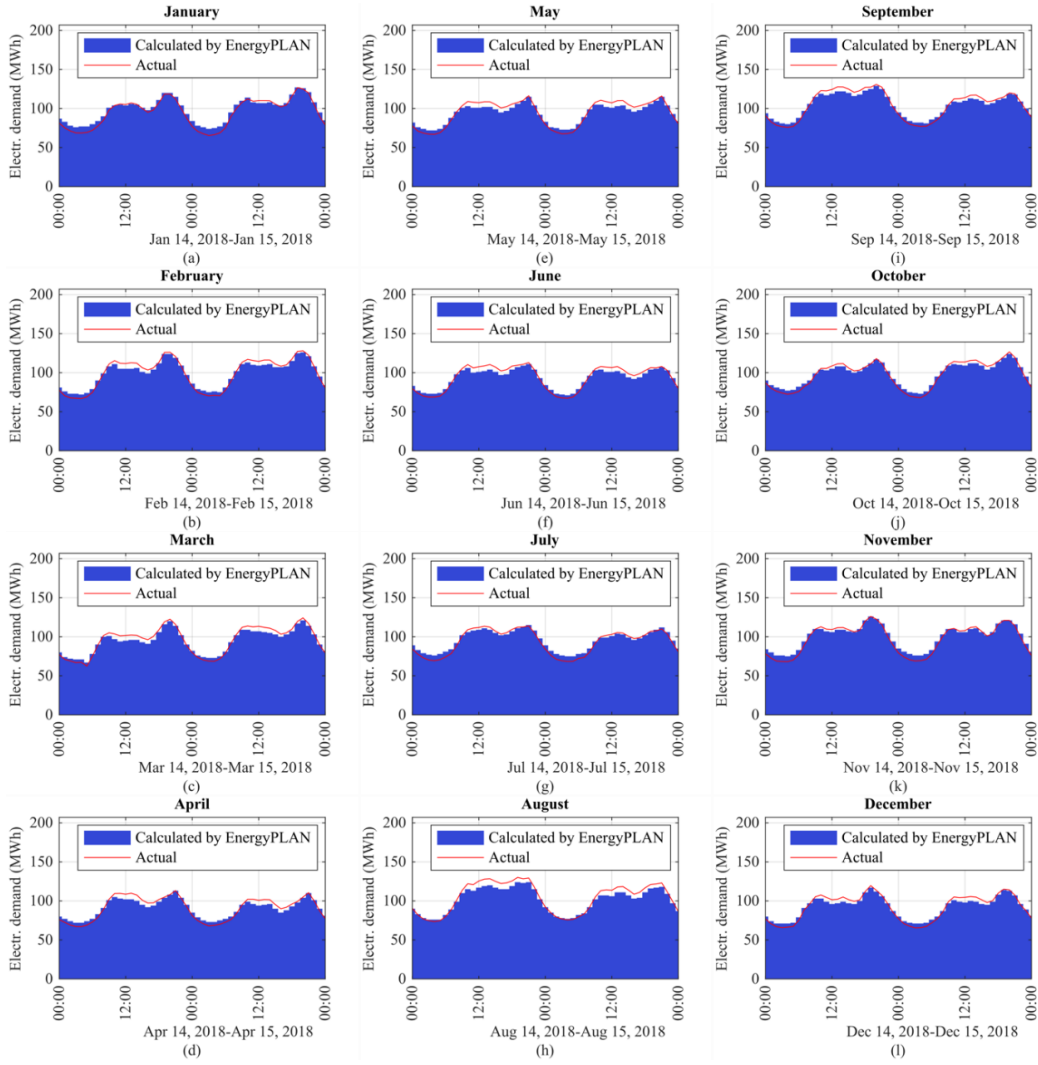
522 electricity systems. However, the EnergyPLAN model analyses this specific power  
523 consumption separately from the electricity sector and achieves a similar water production with  
524 slightly fewer energy resources.

525 **Table 4:** Peak of electrical power obtained from the EnergyPLAN model and actual values for the year 2018 in  
526 Lanzarote.

Month	Actual 2018 (MW)	EnergyPLAN 2018 (MW)	Difference (MW)	Difference (%)
January	136.17	136.00	-0.17	-0.12
February	140.90	138.00	-2.90	-2.06
March	125.80	123.00	-2.80	-2.23
April	119.42	118.00	-1.42	-1.19
May	118.67	117.00	-1.67	-1.40
June	118.63	114.00	-4.63	-3.91
July	123.85	122.00	-1.85	-1.49
August	130.12	124.00	-6.12	-4.70
September	135.17	132.00	-3.17	-2.34
October	132.68	130.00	-2.68	-2.02
November	126.77	126.00	-0.77	-0.60
December	135.85	132.00	-3.85	-2.83
<b>Peak electricity power (MW):</b>	<b>128.67</b>	<b>126.00</b>	<b>-2.67</b>	<b>-2.07</b>

527  
528 Table 4 shows the differences obtained between the modelled peaks of electrical power  
529 generated by months and their actual values. In this case, the maximum differences are detected  
530 in summer months, when renewable resources are higher. In these circumstances, EnergyPLAN  
531 reduces the power contribution of conventional generation taking advantage of the maximum  
532 renewable energy resource.

533 Fig. 12 shows a sample representation of the electricity demand data of the 2018 Lanzarote  
534 energy system and the simulation performed by EnergyPLAN at a 1-h time resolution for the  
535 central days in the months.



536  
537 **Fig. 12.** Sample representation of the behavior of actual 2018 hourly electricity demand and 2018 hourly  
538 electricity demand calculated by EnergyPLAN, for days 14-15 in each month.

539 In Fig. 13, the abscissa axis represents the estimations of electricity demand (measured in  
540 MWh) performed by EnergyPLAN. The ordinate axis represents the actual values observed for  
541 each estimation carried out by the model. Consequently, interceptions between actual and  
542 estimated values are obtained for each sample of data (represented by blue asterisks). The red  
543 line (with a slope of 45 degrees) represents the best possible estimation. A blue asterisk above  
544 the red line means that the observed and estimated values are equal and that a perfect match has  
545 been achieved between model and reality in that individual estimation. In this figure, it can be  
546 seen that there are small differences between estimations and actual values. These  
547 differences were statistically quantified using three metrics: the Mean Absolute Error (MAE),  
548 the Mean Absolute Percentage Error (MAPE) and R-Squared.

549 MAE is defined by Eq. (5) where the  $n$  estimated values are represented by the letter "e" and  
550 the  $n$  observed values by the letter "o". MAE is expressed in the same units as the parameters it  
551 compares [67].

$$MAE = \frac{1}{n} \sum_{i=1}^n |o_i - \hat{e}_i| \quad (5)$$

552 MAPE is defined by Eq. (6) and is a relative measurement that expresses the error as a  
553 percentage of the observed data [67].

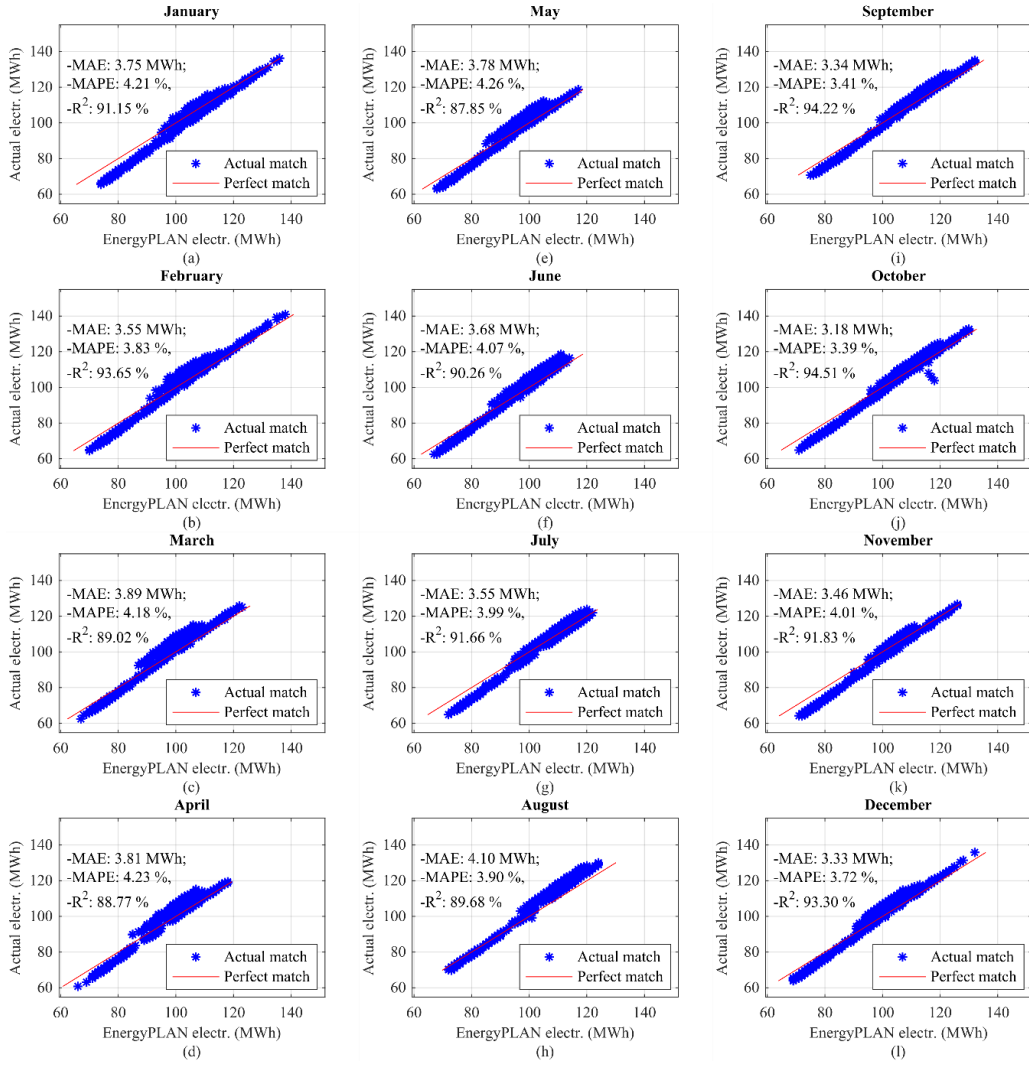
$$MAPE = \frac{100}{n} \sum_{i=1}^n \left| \frac{o_i - \hat{e}_i}{o_i} \right| \quad (6)$$

554 R-Squared is defined by Eq. (7) and indicates the proportionate amount of variation in the  
555 response variable, y, explained by the independent variables, x [68].

556

$$R^2 = \frac{SSR}{SST} \cdot 100 = \left( 1 - \frac{SSE}{SST} \right) \cdot 100 \quad (7)$$

557 where SSE is the sum of squared errors, SSR is the sum of squared regression and SST is the  
558 sum of squared total.



559  
560 **Fig. 13.** Statistical comparison between actual 2018 hourly electricity demand and 2018 hourly electricity  
561 demand calculated by EnergyPLAN.  
562

563 **Table 3:** Electricity produced for Lanzarote in 2018 and the EnergyPLAN simulation for this data.

Production unit	2018 Production (GWh)	EnergyPLAN 2018 (GWh)	Difference (TWh)	Difference (%)
Power-plants	926.20	943.98	17.78	1.9%
Wind	50.96	50.95	-0.01	0.0%
PV	9.50	9.43	-0.07	-0.7%

564

565

566 **Table 4:** Electricity produced for Lanzarote in 2018 and the EnergyPLAN simulation for this data.

Fuel	2018 Fuel consumption (GWh)	EnergyPLAN fuel consumption 2018 (GWh)	Difference (GWh)	Difference (%)
Oil	3,441.78	3,430.00	-11.780	-0.3%
Natural gas	103.500	100.00	-3.500	-3.5%
Renewable	60.458	60.38	-0.078	-0.1%

567

568 After all the comparisons between the reference model and the actual 2018 data had been  
 569 completed and analysed, the accuracy of the model was accepted. As the largest relative  
 570 difference found was just 4.7%, the reference model of the existing energy system of Lanzarote  
 571 can be used as the first step for the investigation carried out in this paper.

572 **3.4 Smart energy-water infrastructures analysis and Pareto-based optimization**

573 After validation of the Lanzarote reference model, step 4 in the process was carried out. A  
 574 MATLAB program was developed to obtain the optimal renewable water infrastructures using  
 575 the framework shown in Fig. 3, the detailed method described in Fig. 4 and the Pareto-based  
 576 optimization model presented in Section 2.4.

577 This Pareto-based optimization model is specifically formulated as follows:

$$\begin{aligned}
 \text{minimize:} \quad & y_1 = \text{total annual } CO_2 \text{ emissions (Mt)}, \\
 & y_2 = 100\% - \text{RES share of PES (\%}), \\
 & y_3 = \text{total annual fuel consumption, PES, (TWh)}, \\
 & y_4 = \text{total annual oil contribution to PES (TWh)}, \\
 & y_5 = \text{maximum required hourly import (MW)}, \\
 & y_6 = \text{imports/exports intersection point (TWh)}, \\
 & y_7 = \text{annual variable costs (M\text{\euro})}, \\
 & y_8 = \text{total annual costs (M\text{\euro})}, \\
 \\
 \text{subject to:} \quad & 0.243 \text{ hm}^3 \leq x_1 \leq 24.3 \text{ hm}^3, \\
 & 4000 \text{ m}^3/\text{h} \leq x_2 \leq 8000 \text{ m}^3/\text{h}, \\
 & 22.3 \text{ MW} \leq x_3 \leq 379.74 \text{ MW}, \\
 & 9 \text{ MW} \leq x_4 \leq 475 \text{ MW}
 \end{aligned} \tag{8}$$

$$\begin{aligned}
 \text{where:} \quad & x_1 = \text{water storage capacity (Mm}^3\text{)}, \\
 & x_2 = \text{desalinated water production capacity (1000 m}^3/\text{h}), \\
 & x_3 = \text{wind power installed capacity (MW)} \\
 & x_4 = \text{PV power installed capacity (MW)}
 \end{aligned}$$

578 In this study, the decision variables (water storage capacity, desalination water capacity, wind  
579 power capacity installed in the energy system and PV power capacity) were modified on the  
580 basis of the following criteria:

581 a) Water storage capacity: in 10 steps, from its 2018 installed capacity ( $0.243 \text{ hm}^3$ ) to 100  
582 times this value ( $24.3 \text{ hm}^3$ ).

583 b) Total water desalination capacity: in 10 steps, from its 2018 installed capacity ( $4000 \text{ m}^3/\text{h}$ ) to 8000  $\text{m}^3/\text{h}$ .

585 c) Wind power capacity: in 10 steps of equal increments, from its 2018 installed capacity  
586 ( $22.3 \text{ MW}$ ) to the value which would satisfy all the electricity demand with this kind of  
587 power ( $379.74 \text{ MW}$ ).

588 d) PV power capacity: in 10 steps, from its 2018 installed capacity ( $9 \text{ MW}$ ) to the value  
589 which would satisfy all the electricity demand with this kind of power ( $475 \text{ MW}$ ).

590 The same general procedure was applied to determine the minimum intersection point between  
591 imports, i.e. fossil fuel energy needs, and exports, i.e. excess electricity production (EEP), in  
592 each water infrastructure when wind and PV are increased sequentially. This intersection point  
593 is important for any future development of the energy system as it defines the energy storage  
594 size required to minimize fossil fuel consumption. For each water infrastructure configuration  
595 (water storage and desalination capacity binomial), a search was performed for the optimal  
596 wind/PV power capacity configuration. This procedure was carried out in MATLAB using the  
597 MATLAB Toolbox for EnergyPLAN [20].

598

599

600 **4 Results and discussion**

601 Table 5 shows a sample of the results obtained and, more specifically, the following data  
602 gathered from the EnergyPLAN output files:

- 603 – Desalinated water production capacity (1000 m<sup>3</sup>/h).
- 604 – Water storage capacity (Mm<sup>3</sup>).
- 605 – PV power capacity required (MW) and in percentage (%) of total electricity demand.
- 606 – Wind power capacity required (MW) and in percentage (%) of total electricity demand.
- 607 – Total annual CO<sub>2</sub> emissions (Mt).
- 608 – RES share of PES (%).
- 609 – Total annual PES (TWh).
- 610 – Total annual oil contribution to PES (TWh).
- 611 – Maximum required hourly import (MW).
- 612 – Import/export intersection value, in TWh and in percentage (%) of total electricity demand.
- 613 – Variable costs of the energy system, in millions of euros (M€).
- 614 – Total annual costs of the energy system, in M€.

615 All the optimal feasible solutions shown in Table 5 are also represented in three charts (Fig. 14  
616 a, b and c) using only two potentially conflicting target variables in each. More specifically,  
617 Fig. 14a shows the results of the optimal solutions in terms of total annual costs (M€) vs. total  
618 annual fuel consumption (TWh), Fig. 14b represents the obtained solutions in terms of total  
619 annual costs vs. annual CO<sub>2</sub> emissions (Mt), and Fig. 14c shows total annual costs for the  
620 solutions vs. import/export intersection values (TWh), which are equivalent to the annual  
621 energy storage needs to avoid fossil fuels in the system. In Fig. 14, the three Pareto fronts are  
622 represented by discontinuous lines.

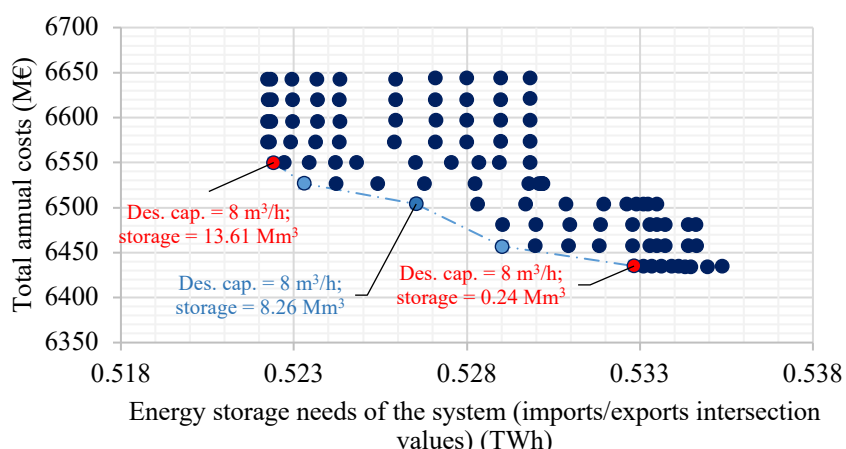
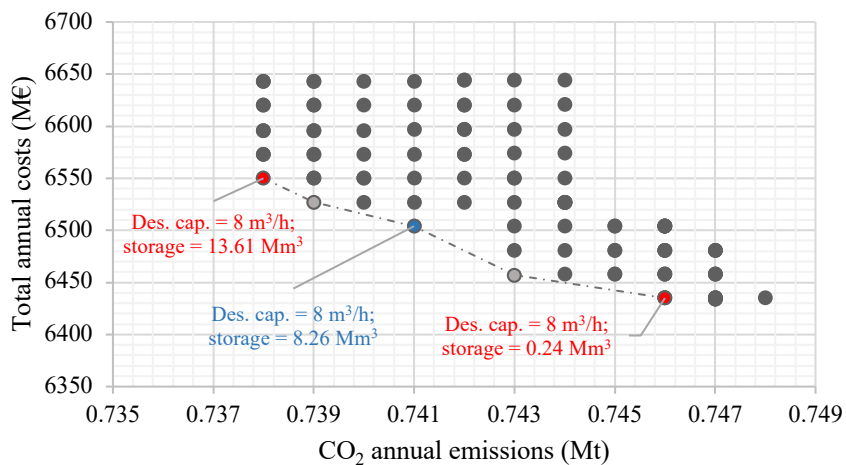
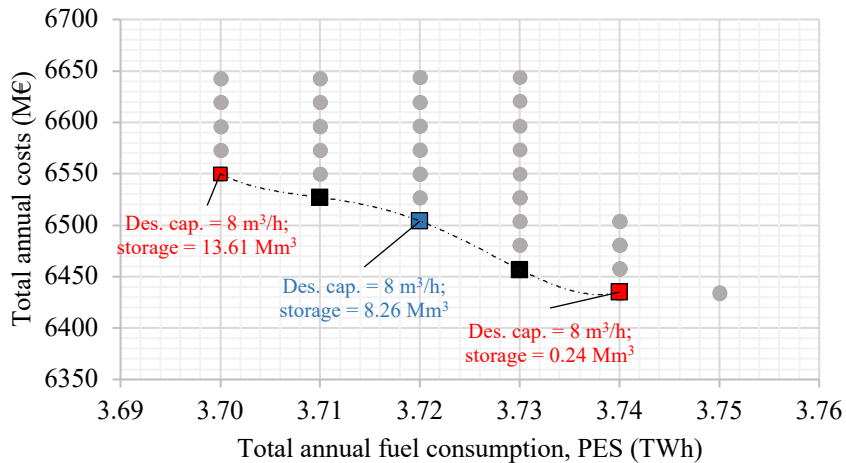
623

624

**Table 5:** Representative sample of the total set of optimal feasible smart energy-water infrastructures obtained after applying the proposed method on the island of Lanzarote.

Desal. cap.	Water storage	PV power	Wind power		CO <sub>2</sub>	RES of PES	Total annual PES	Total annual oil	Max Imports	Import/Export	Var. Costs	Total annual costs		
1000 m <sup>3</sup> /h	Mm <sup>3</sup>	MW	%	MW	%	Mt	%	TWh	TWh	M€	TWh	%	M€	M€
<b>4.00</b>	<b>0.24</b>	<b>9</b>	<b>2</b>	<b>22.30</b>	<b>5.87</b>	<b>0.929</b>	<b>5.14</b>	<b>3.59</b>	<b>3.40</b>	<b>133</b>	<b>0.78</b>	<b>92.86</b>	<b>201</b>	<b>6424</b>
4.00	0.24	95	20	272.28	71.70	0.748	24.5	3.75	2.73	137	0.535	63.68	167	6435
4.00	2.92	95	20	272.30	71.71	0.747	24.5	3.74	2.73	137	0.534	63.59	167	6458
4.00	5.59	95	20	272.30	71.71	0.747	24.5	3.74	2.73	137	0.534	63.59	167	6481
⋮	⋮	⋮	⋮	⋮	⋮	⋮	⋮	⋮	⋮	⋮	⋮	⋮	⋮	⋮
4.44	8.26	95	20	272.23	71.69	0.746	24.5	3.74	2.73	137	0.533	63.45	167	6504
4.44	10.94	95	20	270.66	71.27	0.744	24.5	3.73	2.72	137	0.530	63.05	166	6527
4.44	13.61	95	20	269.12	70.87	0.743	24.4	3.72	2.71	136	0.528	62.91	166	6550
⋮	⋮	⋮	⋮	⋮	⋮	⋮	⋮	⋮	⋮	⋮	⋮	⋮	⋮	⋮
4.89	16.28	95	20	268.77	70.78	0.742	24.4	3.72	2.71	136	0.527	62.80	166	6573
4.89	18.95	95	20	268.78	70.78	0.742	24.4	3.72	2.71	136	0.527	62.80	166	6597
4.89	21.63	95	20	268.78	70.78	0.742	24.4	3.72	2.71	136	0.527	62.80	166	6620
⋮	⋮	⋮	⋮	⋮	⋮	⋮	⋮	⋮	⋮	⋮	⋮	⋮	⋮	⋮
5.33	24.30	95	20	268.71	70.76	0.742	24.5	3.72	2.71	136	0.527	62.69	166	6644
5.78	0.24	95	20	272.30	71.71	0.747	24.5	3.74	2.73	137	0.534	63.53	167	6435
5.78	2.92	95	20	272.29	71.70	0.746	24.5	3.74	2.73	137	0.533	63.43	167	6458
⋮	⋮	⋮	⋮	⋮	⋮	⋮	⋮	⋮	⋮	⋮	⋮	⋮	⋮	⋮
6.22	5.59	95	20	272.32	71.71	0.746	24.5	3.74	2.73	137	0.532	63.37	167	6481
6.22	8.26	95	20	272.18	71.67	0.745	24.5	3.74	2.72	137	0.531	63.27	167	6504
6.22	10.94	95	20	271.02	71.37	0.743	24.5	3.72	2.71	137	0.528	62.83	166	6527
⋮	⋮	⋮	⋮	⋮	⋮	⋮	⋮	⋮	⋮	⋮	⋮	⋮	⋮	⋮
7.11	13.61	95	20	269.25	70.90	0.739	24.5	3.71	2.70	136	0.523	62.25	165	6550
7.11	16.28	95	20	268.42	70.69	0.739	24.5	3.70	2.70	136	0.522	62.19	165	6573
7.11	18.95	95	20	268.49	70.70	0.739	24.5	3.70	2.70	136	0.522	62.20	165	6596
⋮	⋮	⋮	⋮	⋮	⋮	⋮	⋮	⋮	⋮	⋮	⋮	⋮	⋮	⋮
7.56	21.63	95	20	268.48	70.70	0.738	24.5	3.70	2.70	136	0.522	62.12	165	6620
7.56	24.30	95	20	268.47	70.70	0.738	24.5	3.70	2.70	136	0.522	62.12	165	6643
<b>8.00</b>	<b>0.24</b>	<b>95</b>	<b>20</b>	<b>272.60</b>	<b>71.79</b>	<b>0.746</b>	<b>24.5</b>	<b>3.74</b>	<b>2.73</b>	<b>137</b>	<b>0.532</b>	<b>63.37</b>	<b>167</b>	<b>6435</b>
8.00	2.92	95	20	272.30	71.71	0.743	24.6	3.73	2.71	137	0.529	62.92	166	6457
8.00	5.59	95	20	272.17	71.67	0.743	24.6	3.73	2.71	137	0.529	62.92	166	6481
<b>8.00</b>	<b>8.26</b>	<b>95</b>	<b>20</b>	<b>271.99</b>	<b>71.62</b>	<b>0.741</b>	<b>24.6</b>	<b>3.72</b>	<b>2.71</b>	<b>137</b>	<b>0.526</b>	<b>62.62</b>	<b>166</b>	<b>6504</b>
8.00	10.94	95	20	270.45	71.22	0.739	24.6	3.71	2.70	136	0.523	62.24	165	6527
<b>8.00</b>	<b>13.61</b>	<b>95</b>	<b>20</b>	<b>268.94</b>	<b>70.82</b>	<b>0.738</b>	<b>24.6</b>	<b>3.70</b>	<b>2.70</b>	<b>136</b>	<b>0.522</b>	<b>62.13</b>	<b>165</b>	<b>6550</b>
8.00	16.28	95	20	268.57	70.73	0.738	24.5	3.70	2.70	136	0.522	62.11	165	6573
8.00	18.95	95	20	268.64	70.74	0.738	24.5	3.70	2.70	136	0.522	62.11	165	6596
8.00	21.63	95	20	268.67	70.75	0.738	24.5	3.70	2.70	136	0.522	62.11	165	6620
8.00	24.30	95	20	268.65	70.75	0.738	24.5	3.70	2.70	136	0.522	62.11	165	6643

\* **in bold** are represented the results obtained for the reference scenario.\* **in red** are represented the optimal configurations situated in the extremes of the Pareto fronts.\* **in blue** is represented the trade-off Pareto-optimal solution.



636 **Fig. 14.** Optimal solutions and Pareto fronts shown as total annual costs (M€) vs.: a) Total annual fuel  
637 consumption (TWh); b) CO<sub>2</sub> annual emissions and; c) Annual energy storage needs to minimize fossil fuels in  
638 the system (import/export intersection value).  
639  
640

641 Shown in blue in Fig. 14 and Table 5 is the most balanced energy-water infrastructure obtained  
642 after applying the proposed method to the island of Lanzarote. It is based on:

643 – a desalination capacity of 8,000 m<sup>3</sup>/h,  
644 – a water storage capacity of 8.26 M m<sup>3</sup>,  
645 – an installed PV power capacity of 95 MW, capable of satisfying 20% of total electricity  
646 demand, and  
647 – an installed wind power capacity of 271.99 MW, capable of satisfying 71.62% of total  
648 electricity demand.

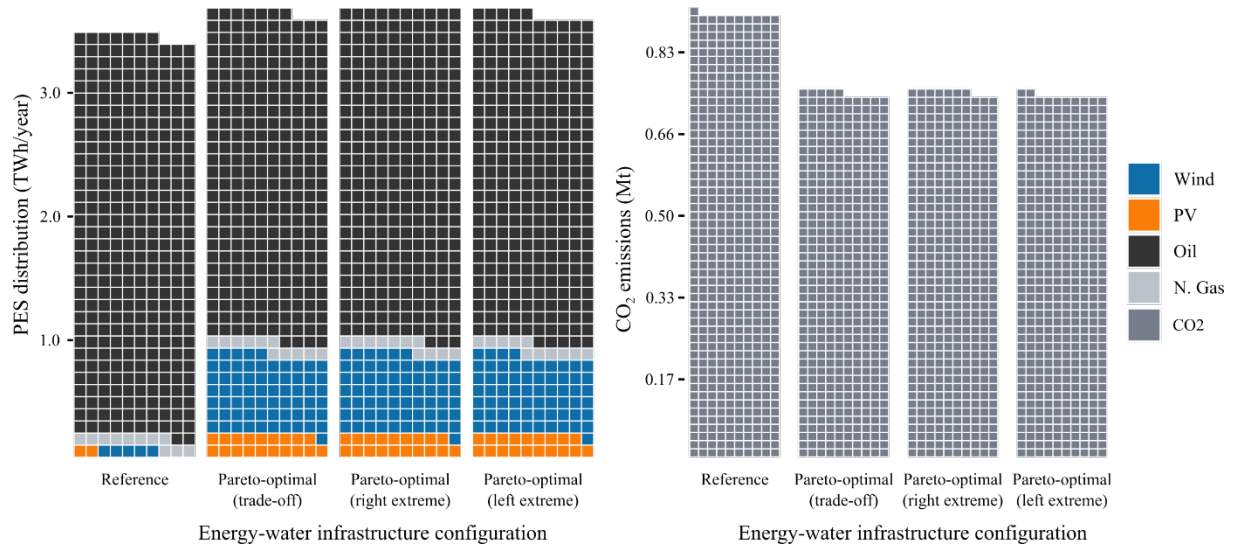
649 This configuration would increase the participation of renewables in the primary energy supply  
650 of the energy system from the current 5.14% of the reference energy system to 24.6%. This  
651 corresponds to, on average, over 35% of the hourly electricity demand throughout 2018 being  
652 satisfied by renewables compared to the actual value of 6.6%, with maximum hourly renewable  
653 contributions of up to 65%.

654 It can be seen that the optimal solutions generally propose a PV/wind power combination based  
655 on 20% of annual electricity demand being satisfied by PV and 71.62% by wind. These results  
656 concur with conclusions obtained in previous studies which analysed the best PV/wind power  
657 combination [3,69,70] with a view to minimizing excess electricity problems.

658 Fig. 15 shows the PES distribution and CO<sub>2</sub> emissions for the three Pareto-optimal solutions  
659 (located in the extremes and the center of the Pareto front) and for the reference scenario. For  
660 the trade-off Pareto-optimal scenario, despite the increase in total PES (from 3.59 to 3.72  
661 TWh/year), the total oil contribution to the PES is reduced from 3.40 TWh/year to 2.71  
662 TWh/year. Importantly, wind and PV power contributions are considerably increased, and  
663 annual CO<sub>2</sub> emissions reduced from 0.929 Mt to 0.741 Mt.

664

PES distribution and CO<sub>2</sub> emissions  
for the Pareto-optimal configurations and the reference scenario



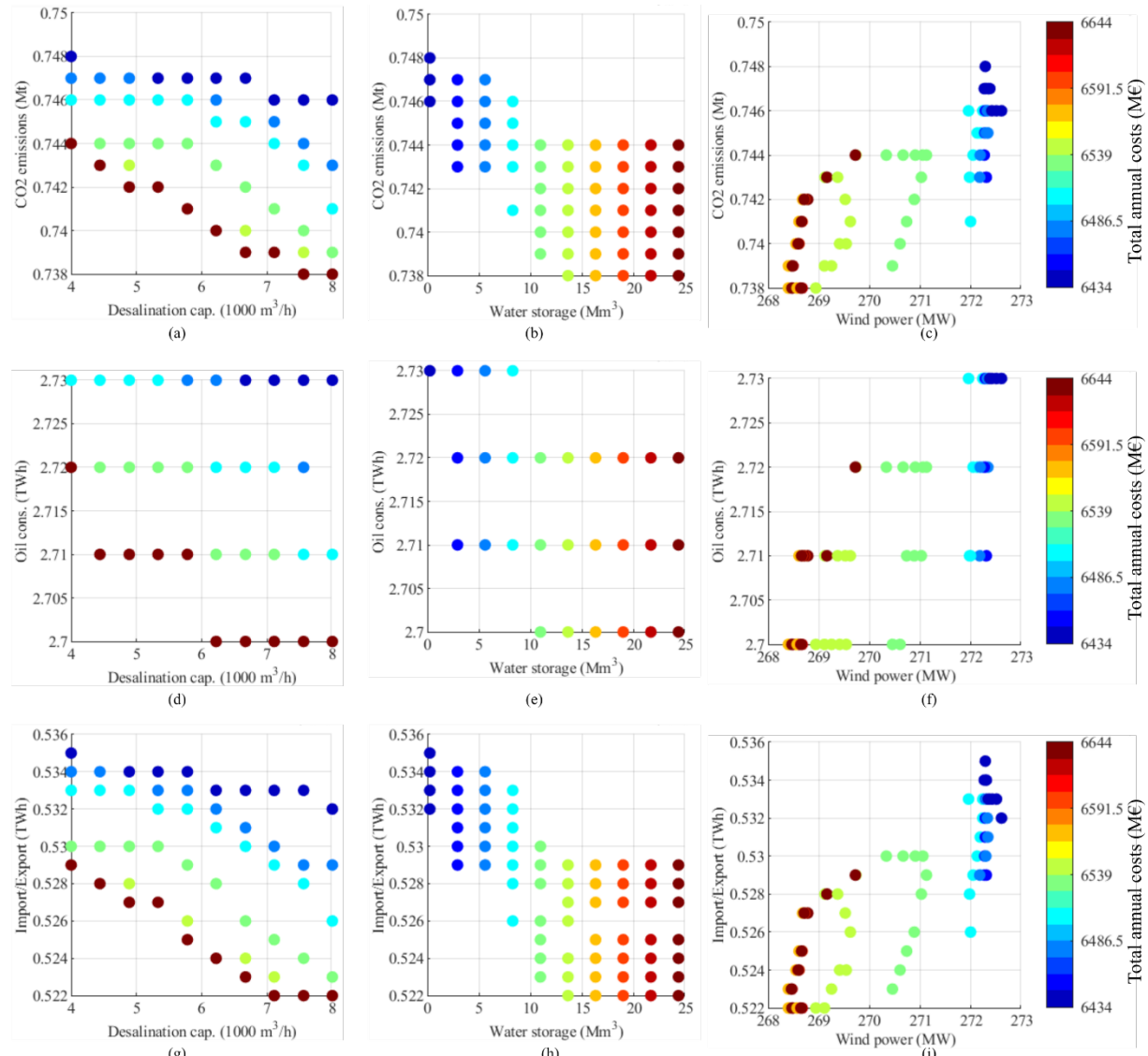
665  
666 **Fig. 15.** PES distribution and CO<sub>2</sub> emissions for the reference scenario and the optimal configurations obtained  
667 in the Pareto front.

668  
669 In Fig. 16, the optimal solutions are represented in terms of installed desalination, water storage  
670 and wind power capacities (X-axis), and CO<sub>2</sub> emissions, oil consumption and import/export  
671 intersection (Y-axis). Additionally, all the optimal solutions are drawn using a color code  
672 corresponding to their total annual cost.

673 The solutions with the lowest CO<sub>2</sub> emissions have higher total annual costs (Fig. 16a). This is  
674 because to satisfy the criteria of low CO<sub>2</sub> emissions and high desalination capacity it was  
675 necessary to increase water storage to its highest values, which significantly increased the total  
676 costs in the system.

677 All the graphs plotted in the second column of Fig. 16 offer confirmation of this. In this respect,  
678 it could be inferred that, in general terms, lower water storage capacity implies a lower total  
679 cost in the system. However, Fig. 16 (a), (d) and (g) show optimal solutions in green with very  
680 good performances in terms of the import/export intersection obtained on the basis of CO<sub>2</sub>  
681 emissions, total annual costs, oil consumption and import/export intersections. In addition, as  
682 can be seen in Fig. 16 (b), (e) and (h), these good performances were obtained with mid-range

683 water storage solutions. Likewise, Fig. 16 (c), (f) and (i) show that lower total annual costs were  
 684 obtained when wind contributions were higher, but very good performances were obtained with  
 685 mid-range wind power solutions.



686  
 687 **Fig. 16.** Representation of each individual energy-water configuration (solutions) in terms of: desalination  
 688 capacity and total annual costs (first column); water storage and total annual costs (second column); and wind  
 689 power and total annual costs (third column), vs. CO<sub>2</sub> emissions; oil consumption; and import/export intersections  
 690 (energy storage needs).

691

## 692 5 Conclusions

693 In this paper, an overall method is proposed to plan island energy-water infrastructures on the  
 694 basis of the interrelation between the electricity and desalination sectors with the aim of  
 695 increasing the renewable energy contribution to the whole energy system. The method is

696 inspired by the Smart Energy System concept which promotes interconnections between  
697 different sectors to take advantages of their synergies. Since, in principle, the method is focused  
698 on islands, it has been designed to include an optimal renewable configuration search to  
699 minimize the balance between fuel energy needs and electricity excesses.

700 After applying the method to the Lanzarote case study, an island in the Canary Archipelago  
701 (Spain), a number of specific and relevant results were obtained. First, the analyses confirm the  
702 initial hypothesis with respect to the positive potential contribution that flexible desalination  
703 can make to renewable integration in an energy system. As result of the application of the  
704 proposed method, it is concluded that the most appropriate solution —in terms of maximizing  
705 renewable energy contribution and minimizing CO<sub>2</sub> emissions, fossil fuel use and total annual  
706 costs— is a trade-off optimal solution chosen in accordance with the Pareto-efficiency concept.  
707 This solution consists of a balanced energy-water infrastructure based on a bigger but not the  
708 biggest selected water storage capacity, a higher but not the highest selected wind power  
709 capacity, and the highest, in size, selected desalination water capacity. This solution achieves  
710 an increase in the total contribution of renewables from 5.14% in the current reference scenario  
711 to 24.6%. This corresponds to, on average, over 35% of the hourly electricity demand  
712 throughout 2018 being covered by renewables, against the current 6.6%. The optimal solutions  
713 suggested by the method propose a PV/wind power combination based on 20% of annual  
714 electricity demand being satisfied by PV and 71.62% by wind, concurring with conclusions  
715 obtained in previous studies which analysed the best PV/wind power combination with a view  
716 to minimizing excess electricity problems.

717 **Acknowledgements**

718 This research has been co-funded by the ERDF as part of the INTERREG MAC 2014-2020  
719 program [E5DES Project (MAC2/1.1a/309)].

720 **References**

721 [1] Chen F, Duic N, Manuel Alves L, da Graça Carvalho M. Renewislands—Renewable  
722 energy solutions for islands. *Renew Sustain Energy Rev* 2007;11:1888–902.  
723 doi:10.1016/j.rser.2005.12.009.

724 [2] Segurado R, Krajačić G, Duić N, Alves L. Increasing the penetration of renewable  
725 energy resources in S. Vicente, Cape Verde. *Appl Energy* 2011;88:466–72.  
726 doi:10.1016/j.apenergy.2010.07.005.

727 [3] Cabrera P, Lund H, Carta JA. Smart renewable energy penetration strategies on islands:  
728 The case of Gran Canaria. *Energy* 2018;162:421–43. doi:10.1016/j.energy.2018.08.020.

729 [4] Sadhwani J, Veza J. Desalination and energy consumption in Canary Islands.  
730 *Desalination* 2008;168:39–47.

731 [5] El Mansouri A, Hasnaoui M, Amahmid A, Hasnaoui S. Feasibility analysis of reverse  
732 osmosis desalination driven by a solar pond in Mediterranean and semi-arid climates.  
733 *Energy Convers Manag* 2020;221:113190. doi:10.1016/j.enconman.2020.113190.

734 [6] Segurado R, Costa M, Duić N. Integrated Planning of Energy and Water Supply in  
735 Islands. *Renew. Energy Powered Desalin. Handb. Appl. Thermodyn.*, Elsevier Inc.;  
736 2018, p. 331–74. doi:10.1016/B978-0-12-815244-7.00009-X.

737 [7] Elmaadawy K, Kotb KM, Elkadeem MR, Sharshir SW, Dán A, Moawad A, et al.  
738 Optimal sizing and techno-enviro-economic feasibility assessment of large-scale reverse  
739 osmosis desalination powered with hybrid renewable energy sources. *Energy Convers  
740 Manag* 2020;224:113377. doi:10.1016/j.enconman.2020.113377.

741 [8] Charcosset C. A review of membrane processes and renewable energies for desalination.  
742 *Desalination* 2009;245:214–31. doi:<http://dx.doi.org/10.1016/j.desal.2008.06.020>.

743 [9] Qingfen M, Hui L. Wind energy technologies integrated with desalination systems:  
744 Review and state-of-the-art. *Desalination* 2011;277:274–80.  
745 doi:10.1016/J.DESAL.2011.04.041.

746 [10] Carta JA, González J, Cabrera P, Subiela VJ. Preliminary experimental analysis of a  
747 small-scale prototype SWRO desalination plant, designed for continuous adjustment of  
748 its energy consumption to the widely varying power generated by a stand-alone wind  
749 turbine. *Appl Energy* 2015;137:222–39. doi:10.1016/j.apenergy.2014.09.093.

750 [11] Gómez-Gotor A, Del Río-Gamero B, Prieto Prado I, Casañas A. The history of  
751 desalination in the Canary Islands. *Desalination* 2018;428:86–107.  
752 doi:10.1016/j.desal.2017.10.051.

753 [12] Piernavieja G, Veza JM, Padrón JM. Experience in desalination training and know-how

754 in the Canary Islands. *Desalination* 2001;141:205–8. doi:10.1016/S0011-  
755 9164(01)00405-2.

756 [13] Cabrera P, Carta JA. Computational Intelligence in the Desalination Industry, Springer,  
757 Cham; 2019, p. 105–31. doi:10.1007/978-3-030-25446-9\_5.

758 [14] Cabrera P, Carta JA, González J, Melián G. Artificial neural networks applied to manage  
759 the variable operation of a simple seawater reverse osmosis plant. *Desalination*  
760 2017;416:140–56. doi:10.1016/j.desal.2017.04.032.

761 [15] Al Aani S, Bonny T, Hasan SW, Hilal N. Can machine language and artificial  
762 intelligence revolutionize process automation for water treatment and desalination?  
763 *Desalination* 2019;458:84–96. doi:10.1016/j.desal.2019.02.005.

764 [16] González J, Cabrera P, Carta JA. Wind Energy Powered Desalination Systems. *Desalin.*  
765 Water from water. 2nd ed., Hoboken, NJ, USA: John Wiley & Sons, Inc.; 2019, p. 567–  
766 646. doi:10.1002/9781119407874.ch14.

767 [17] Aguilar RM, Torres JM, Martín CA. Automatic learning for the system identification. A  
768 case study in the prediction of power generation in a wind farm. *RIAI - Rev Iberoam*  
769 *Autom e Inform Ind* 2019;16:114–27. doi:10.4995/riai.2018.9421.

770 [18] Zhang Y, Pan G, Zhao Y, Li Q, Wang F. Short-term wind speed interval prediction based  
771 on artificial intelligence methods and error probability distribution. *Energy Convers*  
772 *Manag* 2020;224:113346. doi:10.1016/j.enconman.2020.113346.

773 [19] Lund H, Thellufsen JZ, Sorknæs P, Connolly D, Mathiesen BV, Østergaard PA, et al.  
774 EnergyPLAN. Advanced energy systems analysis computer model. Documentation  
775 V15.0 2019. <https://www.energyplan.eu/training/documentation/> (accessed July 6,  
776 2017).

777 [20] Cabrera P, Lund H, Zinck Thellufsen J, Sorknæs P. The MATLAB Toolbox for  
778 EnergyPLAN: A tool to extend energy planning studies. *Sci Comput Program*  
779 2020;102405. doi:10.1016/j.scico.2020.102405.

780 [21] Lund H, Østergaard PA, Connolly D, Mathiesen BV. Smart energy and smart energy  
781 systems. *Energy* 2017;137:556–65. doi:10.1016/j.energy.2017.05.123.

782 [22] Connolly D, Lund H, Mathiesen BV. Smart Energy Europe: The technical and economic  
783 impact of one potential 100% renewable energy scenario for the European Union. *Renew*  
784 *Sustain Energy Rev* 2016;60:1634–53. doi:10.1016/j.rser.2016.02.025.

785 [23] Lund H. Renewable energy systems: a smart energy systems approach to the choice and  
786 modeling of 100% renewable solutions. 2nd ed. Massachusetts, USA: Academic Press;  
787 2014.

788 [24] Cabrera P, Carta JA, González J, Melián G. Wind-driven SWRO desalination prototype  
789 with and without batteries: A performance simulation using machine learning models.  
790 *Desalination* 2018;435:77–96. doi:10.1016/j.desal.2017.11.044.

791 [25] Connolly D, Lund H, Mathiesen BV, Leahy M. A review of computer tools for analysing  
792 the integration of renewable energy into various energy systems. *Appl Energy*  
793 2010;87:1059–82. doi:10.1016/j.apenergy.2009.09.026.

794 [26] Østergaard PA. Reviewing EnergyPLAN simulations and performance indicator  
795 applications in EnergyPLAN simulations. *Appl Energy* 2015;154:921–33.  
796 doi:10.1016/j.apenergy.2015.05.086.

797 [27] van Beuzekom I, Gibescu M, Slootweg JG. A review of multi-energy system planning  
798 and optimization tools for sustainable urban development. 2015 IEEE Eindhoven  
799 PowerTech, IEEE; 2015, p. 1–7. doi:10.1109/PTC.2015.7232360.

800 [28] Batas Bjelić I, Rajaković N. Simulation-based optimization of sustainable national  
801 energy systems. *Energy* 2015;91:1087–98. doi:10.1016/J.ENERGY.2015.09.006.

802 [29] Mahbub MS, Cozzini M, Østergaard PA, Alberti F. Combining multi-objective  
803 evolutionary algorithms and descriptive analytical modelling in energy scenario design.  
804 *Appl Energy* 2016;164:140–51. doi:10.1016/J.APENERGY.2015.11.042.

805 [30] Prina MG, Cozzini M, Garegnani G, Manzolini G, Moser D, Filippi Oberegger U, et al.  
806 Multi-objective optimization algorithm coupled to EnergyPLAN software: The  
807 EPLANopt model. *Energy* 2018;149:213–21. doi:10.1016/J.ENERGY.2018.02.050.

808 [31] Srinivas N, Deb K. Multiobjective Optimization Using Nondominated Sorting in  
809 Genetic Algorithms. *Evol Comput* 1994;2:221–48. doi:10.1162/evco.1994.2.3.221.

810 [32] Amanifard N, Nariman-Zadeh N, Borji M, Khalkhali A, Habibdoust A. Modelling and  
811 Pareto optimization of heat transfer and flow coefficients in microchannels using GMDH  
812 type neural networks and genetic algorithms. *Energy Convers Manag* 2008;49:311–25.  
813 doi:10.1016/j.enconman.2007.06.002.

814 [33] Prebeg P, Gasparovic G, Krajacic G, Duic N. Long-term energy planning of Croatian  
815 power system using multi-objective optimization with focus on renewable energy and  
816 integration of electric vehicles. *Appl Energy* 2016;184:1493–507.  
817 doi:10.1016/j.apenergy.2016.03.086.

818 [34] Fonseca CM, Fleming PJ. Genetic Algorithms for Multiobjective Optimization:  
819 Formulation, Discussion and Generalization. Citeseer n.d.  
820 <http://citeseerx.ist.psu.edu/viewdoc/download?doi=10.1.1.48.9077&rep=rep1&type=pdf>  
821 (accessed June 3, 2020).

822 [35] Coello CA, Christiansen AD. Multiobjective optimization of trusses using genetic  
823 algorithms. *Comput Struct* 2000;75:647–60. doi:10.1016/S0045-7949(99)00110-8.

824 [36] Ngatchou P, Zarei A, El-Sharkawi MA. Pareto multi objective optimization. Proc. 13th  
825 Int. Conf. Intell. Syst. Appl. to Power Syst. ISAP'05, vol. 2005, 2005, p. 84–91.  
826 doi:10.1109/ISAP.2005.1599245.

827 [37] Zitzler E. Evolutionary Algorithms for Multiobjective Optimization: Methods and  
828 Applications. Swiss Federal Institute of Technology Zurich, 1999.

829 [38] Kalayci CB, Ertenlice O, Akbay MA. A comprehensive review of deterministic models  
830 and applications for mean-variance portfolio optimization. *Expert Syst Appl*  
831 2019;125:345–68. doi:10.1016/j.eswa.2019.02.011.

832 [39] Liu H, Li Y, Duan Z, Chen C. A review on multi-objective optimization framework in  
833 wind energy forecasting techniques and applications. *Energy Convers Manag*  
834 2020;224:113324. doi:10.1016/j.enconman.2020.113324.

835 [40] Quitoras MR, Cabrera P, Campana PE, Rowley P, Crawford C. Towards robust  
836 investment decisions and policies in integrated energy systems planning: Evaluating  
837 trade-offs and risk hedging strategies for remote communities. *Energy Convers Manag*  
838 2021;229:113748. doi:10.1016/j.enconman.2020.113748.

839 [41] Documentation | EnergyPLAN n.d. <http://www.energyplan.eu/training/documentation/>  
840 (accessed April 25, 2018).

841 [42] The Canary Islands Government. Energy statistics for Canary Islands 2020.  
842 <http://www.gobiernodecanarias.org/istac/jaxi->  
843 [istac/menu.do?uripub=urn:uuid:131cf873-66a9-408d-8cfa-537d6be05067](http://www.gobiernodecanarias.org/istac/menu.do?uripub=urn:uuid:131cf873-66a9-408d-8cfa-537d6be05067) (accessed  
844 May 3, 2020).

845 [43] Canary Islands Institute of Statistics (ISTAC) n.d.  
846 <http://www.gobiernodecanarias.org/istac/> (accessed August 20, 2020).

847 [44] Dirección General de Industria y Energía del Gobierno de Canarias. Proyecto Piloto  
848 sobre la caracterización de los usos finales de la energía en diferentes tipos de  
849 consumidores en Canarias. n.d.

850 [45] Benchotelmark Islas Canarias Herramienta de Gestión Energética en Hoteles Informe  
851 del Proyecto Piloto n.d. <http://www.ithotelero.com/wp-content/uploads/2013/10/proyecto16-benchotelmark-canarias.pdf> (accessed June 8,  
852 2017).

853 [46] The Canary Islands Government. Annual energy report for The Canary Islands. 2018.

854 [47] Brown TW, Bischof-Niemz T, Blok K, Breyer C, Lund H, Mathiesen B V. Response to

856        “Burden of proof: A comprehensive review of the feasibility of 100% renewable-  
857        electricity systems” 2017. <http://arxiv.org/abs/1709.05716> (accessed October 6, 2017).

858        [48] Abido MA. A novel multiobjective evolutionary algorithm for environmental/ economic  
859        power dispatch. *Electr Power Syst Res* 2003;65:71–81. doi:10.1016/S0378-  
860        7796(02)00221-3.

861        [49] Lanzarote - Wikipedia n.d. <https://en.wikipedia.org/wiki/Lanzarote> (accessed September  
862        14, 2020).

863        [50] General Administration of Industry and Energy of the Canary Government and General  
864        Foundation of University of La Laguna. Pilot project about the characterization of energy  
865        uses for the different kind of consumers in Canary Islands n.d.  
866        <http://www.gobcan.es/ceic/energia/doc/eficienciaenergetica/pure/caractusosfinales.pdf>  
867        (accessed April 10, 2017).

868        [51] Desalación y producción - Canal Gestión Lanzarote n.d.  
869        <https://www.canalgestionlanzarote.es/gestionamos-el-agua/nuestro-ciclo-integral-del-agua/produccion-desalacion/> (accessed April 30, 2020).

871        [52] La producción de agua potable ascendió a más de 24,5 millones de m<sup>3</sup> - Canal Gestión  
872        Lanzarote n.d. <https://www.canalgestionlanzarote.es/la-produccion-de-agua-potable-en-2018-ascendio-a-mas-de-245-millones-de-m3/> (accessed May 3, 2020).

874        [53] Island Council of Lanzarote. Centro de datos : Agua, energía y residuos n.d.  
875        <http://www.datosdelanzarote.com/muestraFamilias.asp?idFamilia=18> (accessed April  
876        30, 2020).

877        [54] Red Eléctrica de España S.A.U. System Information of the Operator of the System  
878        (ESIOS) n.d.

879        [55] IDECanarias visor 4.5.1 n.d.  
880        <https://visor.grafcan.es/visorweb/default.php?svc=svcStatISTAC&lat=29.069451252856556&lng=-13.635636138888682&zoom=11&lang=es#> (accessed April 30, 2020).

882        [56] Lanzarote Water Council – Public water management institution in Lanzarote n.d.  
883        <http://consorcioagualanzarote.com/> (accessed May 6, 2020).

884        [57] Lanzarote pierde más de la mitad del agua que producen las desaladoras - La Provincia  
885        - Diario de Las Palmas n.d. <https://www.laprovincia.es/lanzarote/2018/06/09/lanzarote-pierde-mitad-agua-producen/1066702.html> (accessed May 6, 2020).

887        [58] Arrecife reduce en más de un 50% las pérdidas en red - Canal Gestión Lanzarote n.d.  
888        <https://www.canalgestionlanzarote.es/arrecife-reduce-en-mas-de-un-50-las-perdidas-en-red/> (accessed May 6, 2020).

890 [59] Distribución - Canal Gestión Lanzarote n.d.  
891 <https://www.canalgestionlanzarote.es/gestionamos-el-agua/nuestro-ciclo-integral-del->  
892 agua/distribucion-2/ (accessed April 30, 2020).

893 [60] Red Eléctrica de España SAU, Red Eléctrica de España S.A.U. System Information of  
894 the Operator of the System (ESIOS). n.d.

895 [61] Longo S, d'Antoni BM, Bongards M, Chaparro A, Cronrath A, Fatone F, et al.  
896 Monitoring and diagnosis of energy consumption in wastewater treatment plants. A state  
897 of the art and proposals for improvement. *Appl Energy* 2016;179:1251–68.  
898 doi:10.1016/j.apenergy.2016.07.043.

899 [62] Consejo Insular de Aguas de Lanzarote n.d.  
900 <https://www.aguaslanzarote.com/planificacion.php#> (accessed April 30, 2020).

901 [63] Energy Styrelsen. Technology data for energy plants. Generation of electricity and  
902 district heating, energy storage and energy carrier generation and conversion. 2012.

903 [64] IDAE - Institute for Diversification and Energy Saving n.d. <https://www.idae.es/>  
904 (accessed July 2, 2020).

905 [65] The Canary Islands Government. EECan25 - Energy Strategy of The Canary Islands  
906 2015-2025 2017.  
907 [http://www.gobcan.es/ceic/energia/temas/planificacion/EECan25\\_DocumentoPreliminar\\_junio2017.pdf](http://www.gobcan.es/ceic/energia/temas/planificacion/EECan25_DocumentoPreliminar_junio2017.pdf) (accessed May 3, 2018).

909 [66] CO2 Prices - Sendeco2 n.d. <https://www.sendeco2.com/es/precios-co2> (accessed July 2,  
910 2020).

911 [67] Carta JA, Cabrera P, Matías JM, Castellano F. Comparison of feature selection methods  
912 using ANNs in MCP-wind speed methods. A case study. *Appl Energy* 2015;158.  
913 doi:10.1016/j.apenergy.2015.08.102.

914 [68] Lozano A, Cabrera P, Blanco-Marigorta AM. Non-linear regression modelling to  
915 estimate the global warming potential of a newspaper. *Entropy* 2020;22:590.  
916 doi:10.3390/E22050590.

917 [69] Thellufsen JZ, Lund H, Sorknæs P, Østergaard PA, Chang M, Drysdale D, et al. Smart  
918 energy cities in a 100% renewable energy context. *Renew Sustain Energy Rev*  
919 2020;129:109922. doi:10.1016/j.rser.2020.109922.

920 [70] Lund H. Large-scale integration of optimal combinations of PV, wind and wave power  
921 into the electricity supply. *Renew Energy* 2006;31:503–15.  
922 doi:10.1016/j.renene.2005.04.008.